SAPIENZA
Università di Roma
Facoltà di Farmacia e Medicina

Dottorato di Ricerca in
MORFOGENESI e INGEGNERIA TISSUTALE

XXIX Ciclo
(A.A. 2015/2016)

New mechanisms involved in the pathogenesis of osteosarcoma

Dottorando
Enrica Urciuoli

Tutor
Dr.ssa Barbara Peruzzi

Coordinator
Prof. Sergio Adamo

Index

1. The Thesis explained

Osteosarcoma is the most common and most often fatal primary bone tumour, especially affecting children and adolescents. It is a highly aggressive tumour that develops mainly in to the long bones and metastasizes primarily to the lung. Osteosarcoma cells are known to establish a crosstalk with resident bone cells leading to a deleterious vicious cycle.
In this context, we hypothesized that osteosarcoma cells can release in the bone microenvironment transforming extracellular vesicles (EVs) involved in regulating the bone cell proliferation and differentiation, thereby promoting the tumour growth (**Figure 1**). EVs are small, intact and heterogeneous membrane vesicles that exchange nucleic acids and proteins between cells, inducing phenotypic, biochemical and genetic changes in target cells.

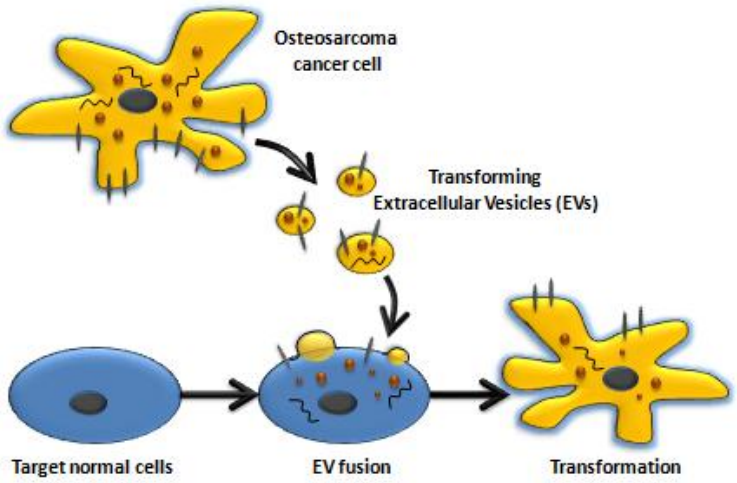

Figure 1. The work hypothesis of this study.

We used human osteosarcoma cell lines to set protocols aimed at isolating, visualizing and characterizing EVs. Our results showed

that osteosarcoma cell lines produce EVs that are able to induce tumour phenotype in recipient murine fibroblasts NIH3T3, as already described for other cancer cell-derived EVs. Indeed, in EV-treated NIH3T3, we observed an enhanced survival capability under low-serum conditions, high levels of activated survival pathways, an increased migration, the acquired capability to grow in an anchorage-independent manner and a *de novo* expression of osteoblastic and tumourigenic markers. As regarding cells of the bone microenvironment, we used human osteoblasts and their precursors (mesenchymal stromal cells), as well as human osteoclasts and their precursors (monocytes), to assess the effects mediated by osteosarcoma-derived EVs. The EV treatment induced an increase of MSC differentiation into mature ALP^+ and Alizarin red^+ osteoblasts. EVs derived from osteosarcoma cells promote the migration and the anchorage-independent growth of normal osteoblasts suggesting a transformation toward a tumour-like phenotype. Finally, monocytes treated with osteosarcoma EVs showed an increased proliferation and the formation of $TRAP^+$ multinucleated osteoclasts, because of presence in EVs of cytokines involved in osteoclast activation and differentiation.
These findings highlight the key role of EVs in the crosstalk between the osteosarcoma and bone microenvironment cells, suggesting that further investigation are needed to better define this new field of research.

2. Introduction

The human skeletal system consists of bones, cartilage, ligaments and tendons and accounts for about 20% of the body weight. The living bones in our bodies use oxygen and give off waste products in metabolism. They contain active tissues that consume nutrients, require a blood supply and change shape or remodel in response to variations in physiology and mechanical stress. Bones provide a rigid framework that supports the body against gravity and protect the soft organs. The adult human skeleton comprises 213 bones, each of which is sculpted by a process called *modelling*, and is constantly renewed by a process termed *remodelling*. Depending on its location, each bone supports one or more specific functions:

- **mechanical**, support and site the muscle attachment for locomotion;
- **protective**, for vital organs and bone marrow;
- **metabolic**, as a reserve of ions, especially calcium and phosphate, for the maintenance of serum homeostasis, which is essential for life. [1]

As in all connective tissues, the fundamental constituents of bone are the cells and the extracellular matrix. The latter is particular abundant and is composed of collagen fibres and non-collagenous proteins. In bone and in the tissue forming the teeth, unlike those in other connective tissues, the matrices have the unique ability to became mineralized (or else have lost the ability to prevent mineralization)[2].

2.1 Bone Tissue

The osteoblast and bone formation

Most of the bone-tissue turnover occurs at the bone surfaces, mainly at the endosteum interfacing with the bone marrow. This surface is morphologically heterogeneous, reflecting the various specific cellular activities involved in remodelling and turnover.
The principal cells that mediate the bone forming processes of the mammalian skeleton are: osteoprogenitor cells, that contribute to maintaining the osteoblast population; osteoblasts, that synthesize the bone matrix on bone forming surfaces; osteocytes, organized throughout the mineralized bone matrix that support bone structure; and the protective bone surface lining cells. The fidelity of bone tissue structure and metabolic functions necessitates exchange of regulatory signals among these cell populations.
Bone formation involves osteoblast maturation that requires a spectrum of signalling proteins including morphogens, hormones, growth factors, cytokines, matrix proteins, transcription factors, and their co-regulatory proteins. They act co-ordinately to support the temporal expression of other genes that represent the phenotypic, structural, and functional properties of osteoblasts during the differentiation process from osteoblast precursors. Osteoprogenitor cells will arise under the appropriate stimulus from stem cells present in many tissues in the adult organism. The bone marrow stroma contains cells with robust proliferative potential that will form single colonies (CFU-Fs) with the capacity to form bone, cartilage, adipocytes and fibroblasts when transplanted *in vivo* in diffusion chambers[3].
These CFU-Fs are now most commonly referred to as *mesenchymal stromal cells* (MSCs) and are distinguished from the hematopoietic stem cell (HSC) lineage. These precursors, with the right stimulation, undergo proliferation and differentiate into pre-osteoblasts and then into mature osteoblasts.

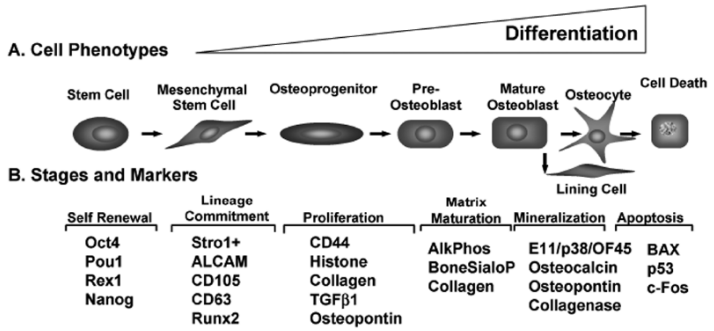

Figure 2. Growth and differentiation of osteoblasts. Schematic illustration of (A) osteoblast lineage cells and (B) frequently used markers of the stages of maturation.

Committed pre-osteoblasts are recognizable near the bone surface by their proximity to surface osteoblasts and by histochemical detection of alkaline phosphatase enzyme activity, one of the earliest markers of the osteoblast phenotype.
The active mature osteoblast on the bone surface is distinguished by its morphological and ultrastructural properties, which are typical of a cell engaged in secretion of a connective tissue matrix, having a large and active nucleus, enlarged Golgi, and extensive rough endoplasmic reticulum.
The osteoblast is highly enriched in alkaline phosphatase and vectorially secretes type I collagen and specialized bone matrix proteins as unmineralized osteoid toward the bone forming front. On quiescent bone surfaces, single layers of flattened osteoblasts or bone lining cells are observed. Osteoblasts and lining cells are in close contact with each other, joined by adherens junctions. Bone matrix synthesis by the osteoblast supports both cell–cell and cell–matrix interactions that are mediated by transmembrane proteins and several classes of adhesion proteins. Integrins, which couple the extracellular matrix to the structural proteins of the cytoskeleton, mediate signals to modulate cell differentiation, cytoskeletal organization, cell adhesion, cell shape change, and cell spreading. The temporal expression of proteins involved in

extracellular matrix biosynthesis and matrix mineralization provides a panel of osteoblast phenotypic markers that reflects stages of osteoblast differentiation (**Figure 2**). Based on bone nodule formation in vitro, the process has been subdivided into three stages:

- proliferation
- extracellular matrix synthesis and maturation
- mineralization, with characteristic changes in gene expression at each stage; apoptosis can also be seen in mature nodules.

Expression of the osteoblast-associated genes type I collagen, alkaline phosphatase, osteopontin, osteocalcin, bone sialoprotein, and PTH/PTH-related protein receptor (PTH1R) is asynchronously upregulated and/or downregulated as the progenitor cells differentiate and matrix matures and mineralizes. In general, alkaline phosphatase and PTH1R are early markers of osteoprogenitors that increase as osteoblasts mature and deposit matrix but decline again with osteoblast transition to osteocytes, whereas osteocalcin is a late marker that is upregulated only in post-mitotic osteoblasts associated with mineralizing osteoid (**Figure 2**). When the pre-osteoblast ceases to proliferate, a key signalling event occurs for development of the large cuboidal differentiated osteoblasts on the bone surface from the spindle shaped osteoprogenitors. The osteoblast is responsible for synthesis of the extracellular matrix (ECM) leading to a "matrix maturation" stage when induced expression of alkaline phosphatase and specialized bone proteins render the ECM competent for mineral deposition. The composition and organization of the bone ECM is critical for structural and functional fidelity of bone tissue for constituents of the ECM. Mineralization results in upregulated expression of several non-collagenous proteins, thereby providing markers of the mature osteoblasts. These calcium and phosphate binding proteins may function in regulating the ordered deposition of mineral, amount of the hydroxyapatite crystals, or crystal size.

The osteoclast and bone resorption

The osteoclast, the exclusive bone resorptive cell, is a member of the monocyte/macrophage family and a polykaryon that can be generated *in vitro* from mononuclear phagocyte precursors resident in a number of tissues[4]. Two cytokines are essential and sufficient for basal osteoclastogenesis, Receptor Activator of Nuclear factor κB ligand (RANKL)[3,5,6] and macrophage colony-stimulating factor (M-CSF). These two proteins, which exist as both membrane-bound and soluble forms, are produced by marrow stromal cells and osteoblasts. RANKL, a member of the TNF superfamily, is the key osteoclastogenic cytokine, because osteoclast formation requires its presence or its priming of precursor cells. M-CSF contributes to the proliferation, survival, and differentiation of osteoclast precursors, as well as the survival and cytoskeletal rearrangement required for efficient bone resorption.. The unique osteoclastogenic properties of RANKL permit generation of pure populations of osteoclasts in culture and hence the performance of meaningful biochemical and molecular experiments that provide insights into the molecular mechanisms by which osteoclasts resorb bone. Key to the resorptive event is the capacity of the osteoclast to form a microenvironment between itself and the underlying bone matrix. This compartment, which is isolated from the general extracellular space, is acidified by an electrogenic proton pump (H^+-ATPase) and a Cl^-/H^+ antiporter to a pH of ~4.5[7]. The acidified milieu mobilizes the mineralized component of bone, exposing its organic matrix, consisting largely of type 1 collagen that is subsequently degraded by the lysosomal enzyme, cathepsin K. Bone resorption also requires a polarization event in which the osteoclast delivers effector molecules like H^+, Cl^- and cathepsin K into the resorptive microenvironment.
Osteoclasts are characterized by a unique cytoskeleton, which mediates the resorptive process. Specifically, when the cell contacts the bone, it generates two polarized structures which enable it to degrade the skeletal tissue. In the first instance, a subset of acidified vesicles containing specific cargo, including

cathepsin K and other matrix metallo-proteases, are transported, probably through microtubules, to the bone-apposed plasma membrane[8], to which they fuse in a manner not currently understood. Insertion of these vesicles into the plasmalemma results in the formation of a villous structure, unique to the osteoclast, the *ruffled membrane*. This resorptive organelle contains the abundant H^+-transporting machinery to create the acidified microenvironment, while the accompanying exocytosis serves as the means by which lysosomal enzymes, including cathepsin K, are secreted. In addition to inducing ruffled membrane formation, contact with bone also prompts the osteoclast to polarize its fibrillar actin into a circular structure known as the *actin ring*. A separate *sealing zone* surrounds and isolates the acidified resorptive microenvironment underneath the active cell, termed resorbing lacuna. The actin ring, like the ruffled membrane, is a hallmark of the degradative capacity of the osteoclast.

Bone remodelling

Remodelling is accomplished by the collaborative and sequential efforts of a group of cells that are collectively termed the *bone remodelling unit* [5].
There are four distinct phases in the remodelling cycle (**Figure 3**):

- activation
- resorption
- reversal
- formation

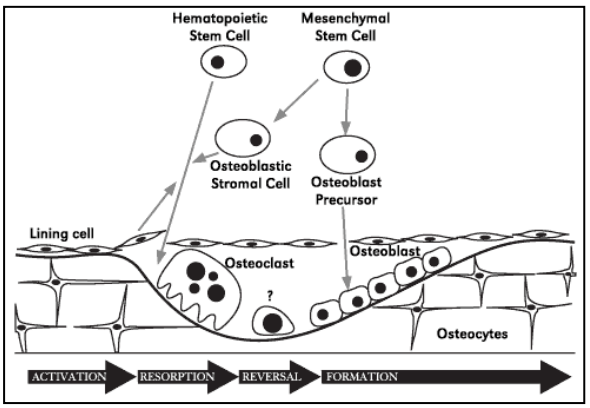

Figure 3. Sequence of the remodelling process. Note that bone is always covered by cells, which are lining cells during quiescent phases.

Activation describes the initiating event that transforms a previously quiescent bone surface into a remodelling one. Activation involves recruitment of mononucleate osteoclast precursors from the circulating monocyte–macrophage lineage[9], infiltration of the bone lining cell layer, and fusion of the mononuclear cells to form multinucleated preosteoclasts (**Figure 3**). The pre-osteoclasts attach themselves to the bone matrix creating an annular sealing zone. In forming the seal, the osteoclast creates the bone-resorbing compartment, a unique microenvironment, between itself and the bone matrix. As described above, osteoclast formation, activation, and activity are all regulated by local cytokines such as RANKL, but also by colony-stimulating factors (CSFs), interleukins-1 and -6 and systemic hormones such as PTH, 1,25-dihydroxyvitamin D3, and calcitonin[9-11]. During the resorption phase of the cycle, specific types of proton pumps in the osteoclast membrane transfer protons to the resorbing compartment considerably lowering its pH. Acidification of the resorbing compartment is accompanied by secretion of a number of lysosomal enzymes, such as tartrate-resistant acid phosphatase (TRAcP) and cathepsin K, as well as matrix metalloproteases including MMP-9 (collagenase)[12].

The acidic solution, containing enzymes that are most active at low pH, effectively dissolves and digests the mineral and organic phases of the matrix, creating saucer-shaped resorption cavities (Howship's lacunae) on the surface of the bone[13]. The resorption phase ends with osteoclast apoptosis[14] and is followed by reversal. During reversal, the resorption lacuna is populated by mononuclear cells, including monocytes, osteocytes that have been liberated from the bone by osteoclasts, and pre-osteoblasts that are being recruited to begin the formation phase of the cycle[15]. It is during the reversal phase that all-important coupling signals are sent out to recruit osteoblasts into the resorption cavities to replace the bone that has been removed. Without an efficient coupling mechanism, each remodelling transaction would result in net loss of bone. Formation is a two-step process in which the osteoblasts initially synthesize the organic matrix and then regulate its mineralization. Once the collagenous organic matrix is secreted, the osteoblasts trigger mineralization by releasing small, membrane-bound vesicles, called matrix vesicles, that establish suitable conditions for initial mineral deposition by concentrating calcium and phosphate ions and enzymatically degrading inhibitors of mineralization, such as pyrophosphate and proteoglycans that are present in the extracellular matrix[16]. As bone formation continues, osteoblasts become entombed in the matrix as osteocytes. Each osteocyte becomes part of a large, 3D, functional syncitium, which can "sense" a change in the mechanical properties of the surrounding bone and transmit this information to the cells on the surface to initiate or regulate bone remodelling when necessary.
The net result of each remodelling cycle is the production of a new osteon in the cortical bone and the replacement of trabeculae in the cancellous bone. Note that the process of bone remodeling is essentially identical in cancellous and cortical bone. The difference between the volume of bone removed by the osteoclasts and that replaced by the osteoblasts is referred to as the "bone balance"[17].

2.2 Bone sarcoma: Osteosarcoma

Clinical aspects of osteosarcoma

Osteosarcoma is the most common primary malignant bone tumour in children and adolescents. Children younger than 5 years are rarely affected; after age 5, the incidence increases with a peak at age 15 years. A second peak occurs in the sixth to seventh decade. This second peak has been associated with Paget disease and prior radiation therapy, although one-half of older osteosarcoma patients have neither condition[18,19]. The adolescent peak occurs at a younger age in girls (13 years) compared with boys (15–17 years), and this corresponds with the age of greatest bone growth. More than 50% of these tumours arise from the long bones around the knee and distal femur, followed by the proximal tibia[20]. Chemotherapy has played a role in the increased overall survival obtained through different clinical trials over the last decades leading to dramatic prognostic improvements in young patients with localized extremity disease, with relapse-free survival rates of approximately 50% to 80%[21]. Metastases at diagnosis are seen in 20% to 25% of patients with OS, with the lung being the most common site. Among patients with nonmetastatic disease at diagnosis, 20% to 25% will relapse, usually in the lungs. For patients with localized tumours, prognosis is better, with an overall event-free survival of 60% to 70%. This survival remains at about 20% to 30% for patients with metastatic disease at diagnosis. In this group, the prognosis seems to be determined by the site, the number of metastases, and their surgical resectability.
The most common clinical presentation of osteosarcoma is pain that becomes continuous and severe with time. This pain is often attributed to recent trauma or bone growth. In some patients, a mass may be palpable and the progressive swelling will affect adjacent joints. Pathologic fractures may occur in osteosarcoma patients either spontaneously or as a result of minimal trauma. Respiratory symptoms from metastatic lung involvement is rare

and require extensive bilateral lung disease. The time between onset of symptoms and diagnosis ranges from 2 to 4 months in developed countries[22]. Some genetic conditions, including Li–Fraumeni syndrome, Paget disease, and some tumours such as retinoblastoma, predispose to develop osteosarcoma[23].

Several prognostic factors affecting overall survival have been identified in patients with osteosarcoma, but these have not been helpful in identifying patients who might benefit from treatment intensification[24]. Some of these prognostic factors include tumour location, tumour size, localized versus metastatic disease, surgical resectability, and degree of tumour necrosis after neoadjuvant chemotherapy. Other possible prognostic factors identified in localized high-grade osteosarcoma include age at diagnosis, serum lactate dehydrogenase level at diagnosis, alkaline phosphatase level, histological subtype, and body mass index at initial presentation. Older patients are considered to do worse secondary to the increased proportion of unfavorable axial lesions with increasing age[24,25].

As regarding tumour location, axial skeleton primary tumours (particularly the pelvis or the spine) are associated with a worse prognosis related to the inability to achieve a complete surgical resection and maintain local control. Within an extremity, a distal tumour location has a more favorable prognosis than a proximal location, secondary to the ability to completely remove the tumour with negative margins. A better prognosis has been documented in patients with head and neck osteosarcoma when compared with extremity tumours, and this may be related to the relatively smaller size of tumours in this anatomic area and a higher proportion of low-grade tumours[25,25-27].

Procurement of adequate diagnostic pathologic specimens is key to determining the correct diagnosis. Once the diagnosis of high-grade osteosarcoma is obtained, neoadjuvant multiagent chemotherapy based on cisplatin, methotrexate, doxorubicin, ifosfamide and etoposide is started[28]. Low-grade osteosarcoma is treated with surgery alone. After the completion of neoadjuvant

chemotherapy, local control with either a limb salvage procedure or an amputation is performed. This procedure involves both the en bloc resection of the tumour and the reconstruction with synthetic materials, biologic materials, or a combination of both. Vascular and nerve reconstruction, muscle flaps, and skin grafts may be necessary[25].

Molecular pathogenesis of osteosarcoma

Several studies highlighted that defects in osteogenic differentiation leading to osteosarcoma development.
Osteoblasts arise from mesenchymal stem cells (MSCs), undifferentiated bone marrow stromal cells with the potential to self-renew and proliferate into bone, muscle, tendon, and fat[29,30]. Milieus of endogenous and exogenous factors are involved in driving the osteogenic pathway from MSC to osteoblast. Dysregulation of these markers, or new exposure to non-native stimuli (e.g. pro-tumour inflammatory cytokines), causes an imbalance between cellular differentiation and proliferation, ultimately contributing to a malignant phenotype.
There are thought to be various similarities between early osteoprogenitors and osteosarcoma cells, including a highly proliferative nature, resistance to apoptosis, and similar expression profiles of genes such as alkaline phosphatase (ALP). Accordingly, more invasive osteosarcoma cells are noted to have minimal expression of osteocalcin (OCN) and osteopontin (OPN), both of which are observed at higher levels in mature osteoblasts.
Bone morphogenetic proteins (BMPs) represent one group of factors involved in osteosarcoma stimulation[31]. Normally involved in carrying MSCs along an osteogenic lineage, BMPs are not only unable to induce differentiation of osteosarcoma cells but may actually promote a more aggressive phenotype[32,33]. This is due to an intrinsic underexpression of Runx2, a transcription factor which usually serves as a master regulator of BMP activity by causing exit from the cell cycle and promoting terminal differentiation[34,35].

However, RUNX2 overexpression is also correlated with poor prognosis of osteosarcoma tumour, indicating that its expression is likely tightly controlled in normal osteogenesis.
As observed in most cancers, abnormal activity of oncogenes and tumour suppressors is a key molecular underpinning of osteosarcoma. MDM2, a protein that marks the tumour suppressor p53 for degradation, is amplified in at least 1 out of 10 patients[36,37]. Furthermore, higher co-expression levels of MDM2 and CDK4, which promotes cell cycle progression, can be used reliably to distinguish low-grade osteosarcoma from benign masses and correlates with further dedifferentiation into high-grade lesions[38-40]. Deficient tumour suppressor activity appears to play an equally important role as dysregulation of oncogenes in osteosarcoma pathogenesis. Rb, a regulator of the G1/S cell cycle transition, is found to be insufficient in about 70% of all sporadic cases of osteosarcoma, not to mention the nearly 1000-fold increased risk for developing osteosarcoma in individuals who inherit an inactivated copy of the gene[41,42]. Similarly, mutations in tumour suppressor p53 are commonly found in osteosarcoma cells and contribute to disease progression by permitting cells with damaged DNA repair mechanisms to evade checkpoints and apoptosis.
Finally, inflammation and cytokine signalling have been heavily implicated in the tumourigenesis of osteosarcoma[43]. For example, transforming growth factor β (TGF-β) is linked to the dedifferentiation of osteosarcoma cells into cancer stem cells, a dynamic population associated with tumour invasion, radio- and chemoresistance, and poor prognosis[44]. Often found to be involved in autocrine signalling by cancer cells, TGF-β increases the migration potential of OS cells through MAPK activation[45]. Similarly, tumour necrosis factor α (TNF-α) is strongly correlated with disease spread, indeed, has been shown to induce MMP-9 in osteosarcoma cells and promote metastasis to lungs *in vivo*[46].

Role of bone microenvironment in osteosarcoma development.

Increasing evidence supports that the bone microenvironment underlies osteosarcoma initiation and progression. Tumour cells may alter the surrounding stroma inducing cell modification and extracellular matrix alteration. In this context, many inflammatory mediators may influence cell proliferation and tumour development, and they are responsible for invasion and immunosuppressive signalling through the production of angiogenic and growth factors, chemokines, cytokines and matrix metalloproteinases.
The expression of various immune mediators and modulators, as well as the abundance and activation state of difference cell types in tumour microenvironment, lead to a tumour-promoting condition. Since tumour cells have a genetically-unstable background, the various factors and cytokines released by such cells might lead to or maintain an altered chronic wound-healing environment that further perpetuates a reactive stroma, leading to enhanced tumour progression and even metastasis[47].

2.3 Extracellular Vesicles (EVs)

Intercellular communication is an essential hallmark of multicellular organisms and can be mediated through direct cell–cell contact or transfer of secreted molecules. In the last two decades, a third mechanism for intercellular communication has emerged that involves intercellular transfer of extracellular vesicles (EVs). Although the release of apoptotic bodies during apoptosis has been long known, the fact that also healthy cells shed vesicles from their plasma membrane has only recently become appreciated. These vesicles are generally referred to as microvesicles, ectosomes, shedding vesicles, or microparticles among others[48,49,50]. The term exosome was initially used for vesicles ranging from 40 to 1,000 nm that are released by a variety of cultured cells[51], but the subcellular origin of these vesicles

remained unclear. Later, this nomenclature was adopted for 40–100-nm vesicles released during reticulocyte differentiation as a consequence of multivesicular endosome (MVE) fusion with the plasma membrane[52]. The involvement of MVEs was demonstrated by the observation that fusion with the plasma membrane released exosomes together with previously endocytosed colloidal gold[53]. Several additional cell types of both hematopoietic and nonhematopoietic origin, such as cytotoxic T cells, platelets, mast cells, neurons, oligodendrocytes, Schwann cells, and intestinal epithelial cells, were also shown to release exosomes through MVE fusion with the cell surface[54,55]. Vesicles with hallmarks of exosomes have been isolated from diverse body fluids, including semen[56,57,58], blood[59], urine[60], saliva[61], breast milk[62], amniotic fluid[63], ascites fluid[64], cerebrospinal fluid[65], and bile[66]. Most of these studies attributed the isolated vesicles to exosomes because of their exosome-like protein contents. However, circulating vesicles are likely composed of both exosomes and microvesicles (MVs), and currently available purification methods, do not allow to fully discriminate between exosomes and MVs. That a single cell type releases both exosomes and MVs has, for example, either been demonstrated or suggested for platelets[67], endothelial cells [68], and breast cancer cells[69]. Confusion on the origin and nomenclature of EVs has spread through the literature as well because vesicles with the size of exosomes that bud at the plasma membrane have also been called exosomes[70]. It should be noted that most studies have not clearly defined the origin of EVs under study; therefore, in this thesis we will mostly refer to EVs rather than MVs or exosomes. A major ongoing challenge is to establish methods that will allow to discriminate between exosomes and MVs. Differences in properties such as size, morphology, buoyant density, and protein composition seem insufficient for a clear distinction[71]. Only when we are able to interfere with the molecular machineries required for EV formation and cargo sequestration will their origins be optimally determined.

Isolation and characterization of EVs

One major challenge in this field is to improve and standardize methods for EV isolation and analysis[72]. Currently, EVs are mostly isolated from the supernatants of cultured cells grown in fetal bovine serum depleted of EVs by performing differential ultracentrifugation. Next, EVs can be efficiently separated from nonmembranous particles, such as protein aggregates, by using their relatively low buoyant density[73,74,75,76] and differences in floatation velocity can be used to separate differently sized classes of EVs[58]. Further characterization of isolated EVs requires complementary biochemical (immunoblotting), mass spectrometry, and imaging techniques, such as electron microscopy. Complementary to electron microscopy, nanoparticle tracking analysis allows determination of the size distribution of isolated EVs based on the Brownian motion of vesicles in suspension[77].

The molecular composition of EVs

The protein content of EVs from different sources has been analyzed by SDS-PAGE followed by protein staining, immunoblotting, or proteomic analysis. Highly purified EVs should be devoid of pollutants, such as serum proteins and protein components of intracellular compartments (e.g., the endoplasmic reticulum or mitochondria), that are never in contact with EVs. As a consequence of their origin, exosomes from different cell types contain endosome-associated proteins (e.g.,Rab GTPase, SNAREs, Annexins, and flotillin), some of which are involved in MVE biogenesis. Membrane proteins that are known to cluster into microdomains at the plasma membrane or at endosomes often are also enriched on EVs. These include tetraspanins, a family of >30 proteins that are composed of four transmembrane domains[78]. Tetraspanins such as CD63, CD81, CD82, CD53, and CD37 were first identified in B cell exosomes[74].

A major breakthrough was the demonstration that the cargo of EVs included both mRNA and miRNA and that EV-associated mRNAs could be translated into proteins by target cells[79,80]. Later studies reported on the RNA contents of EV isolates from other cell cultures[81] and from body fluids[82-84]. EVs with features of exosomes released by immune cells have been demonstrated to selectively incorporate miRNA that can be functionally transferred as a consequence of fusion with recipient cells[85,86]. Analysis of RNA from EVs demonstrated that, in addition to mRNA and miRNA, EVs also contain a large variety of other small noncoding RNA species, including RNA transcripts overlapping with protein coding regions, repeat sequences, structural RNAs, tRNA fragments and small interfering RNAs[87,88]. Many RNAs that were isolated with EVs were found to be enriched relative to the RNA profiles of the originating cells[79-81,88], indicating that RNA molecules are selectively incorporated into EVs. Also, different RNA isolation methods give extensive variation in exosomal RNA yield and patterns[89], and such experimental variations between studies, together with the lack of quantitative data, make it impossible to define a comparative inventory of the RNA species assigned to EVs so far.

Interaction of EVs with recipient cells

Functions of EVs in physiological and pathological processes depend on the ability of EVs to interact with recipient cells and to deliver their contents of proteins, lipids, and RNAs (**Figure 4**).
The cellular and molecular basis for EV targeting is still undetermined, but several target cell–dependent and –conditional aspects are beginning to emerge. Target cell specificity for binding of EVs is likely to be determined by adhesion molecules, such as integrins, that are present in EVs. After binding to recipient cells, EVs may remain stably associated with the plasma membrane or dissociate, directly fuse with the plasma membrane, or be internalized through distinct endocytic pathways (**Figure 4**).

When endocytosed, EVs may subsequently fuse with the endosomal delimiting membrane or be targeted to lysosomes for degradation.
The interest of scientists and physicians in EVs has expanded logarithmically over the past decade in response to the discoveries that EVs are not only generated in cell culture but are also abundantly present in body fluids, carry RNA, and show a wide range of regulatory functions.

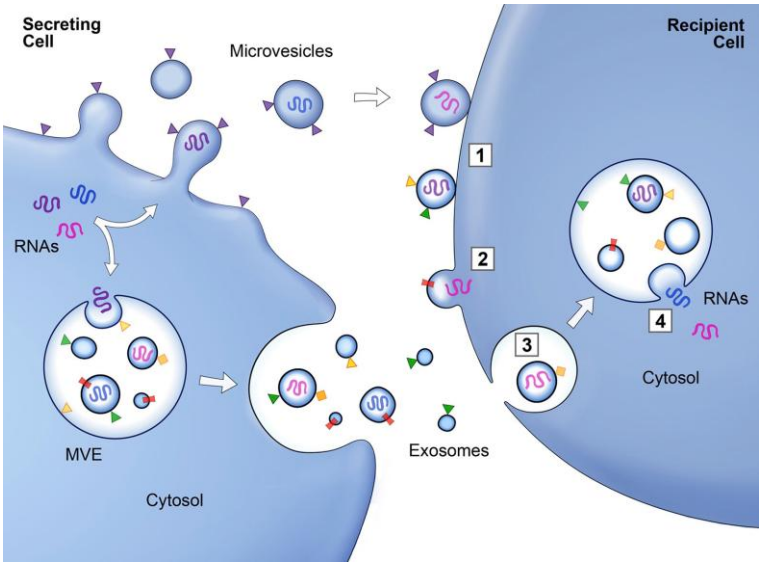

Figure 4. Schematic of protein and RNA transfer by EVs. Membrane-associated (triangles) and transmembrane proteins (rectangles) and RNAs (curved symbols) are selectively incorporated into MVEs budding from the plasma membrane. MVEs fuse with the plasma membrane to elease exosomes into the extracellular milieu. MVs and exosomes may dock at the plasma membrane of a target cell (1). Bound vesicles may either fuse directly with the plasma membrane (2) or be endocytosed (3). Endocytosed vesicles may then fuse with the delimiting membrane of an endocytic compartment (4). Both pathways result in the delivery of proteins and RNA into the membrane or cytosol of the target cell. Fusion and endocytosis are only represented for exosomal vesicles, but plasma membrane–derived MVs may have similar fates[53].

As discussed, we are still at an early stage of deciphering the molecular mechanisms involved in EV biogenesis and recruitment of cargo therein. Specific knowledge of these mechanisms will help us to intervene with EV function in *vivo*, an absolute requirement to decipher their precise role in physiological processes. Also, more accurate and standardised purification methods are required for the implementation in a clinical setting of EVs as biomarkers, vaccines, or drug delivery devices[53].

3. Aims

The field of study based on extracellular vesicle involvement in cancer onset and progression is generating growing interest. Since there are no evidence in the literature regarding this new mechanism of communication in osteosarcoma cancer, the final aim of this thesis is to investigate the role of extracellular vesicles as mediators between cancer cells and resident bone cells.

Therefore, our experimental plan was designed considering three specific aims, as follows:

- To evaluate EV production by osteosarcoma cells
- To assess a tumoral-like conditioning of recipient normal cells mediated by osteosarcoma-derived EVs
- To assess the feasibility to use EVs in therapeutic approaches to osteosarcoma.

4. Results

4.1 Human osteosarcoma cancer cells produce extracellular vesicles.

To evaluate if osteosarcoma cells are able to produce extracellular vesicles (EVs), we used human cell lines to set the best methods for EV isolation and visualization.
Given the variety of EV isolation protocols described in the literature[90], we compared the effectiveness and the reproducibility of 3 different methods for EV collection starting from equal amounts of osteosarcoma cell-conditioned culture medium.
We used osteosarcoma cell lines Saos-2 and 143B, respectively very low aggressive and metastatic cell lines. These cells were stained with two fluorescent dyes, CFSE and PKH-26, to point out respectively green cytoplasms and red plasma membranes, thereby allowing the production of $CFSE^+/PKH\text{-}26^+$ EVs in the conditioned media (**Figure 5)**.

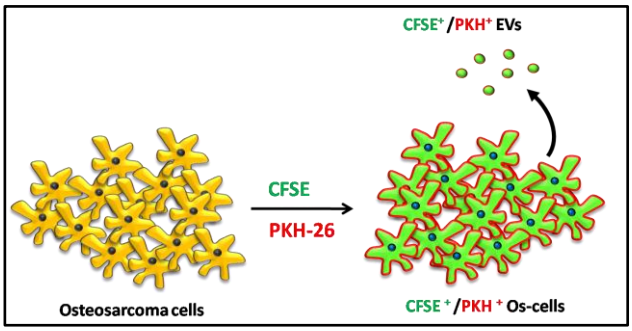

Figure 5. CFSE/PKH-26 staining of osteosarcoma cells

Twenty-four hour conditioned medium was split in 3 equal parts and then processed by using 3 different methods: i) Ultracentrifugation, ii) Amicon Ultra Centrifugal filter and iii) ExoQuick™, a commercial polymer.

Purified EVs were analysed by using fluorescence-activated cell sorting (FACS) for the amount of $CFSE^+/PKH\text{-}26^+$ EVs.
We used beads with a known size of 1.3, 0.7 and 0.5μm to create a gate (size < 1μm) in which we expected to find EVs. Next, we used the fluorescent signal of $CFSE^+$ EVs to distinguish these nanoparticles from background noise (**Figure 6A**), then we analyzed the amount of double positive $CFSE^+/PKH\text{-}26^+$ EVs (**Figure 6B**).
Moreover, to be sure to compare equal volumes, we added the same number of CountBright™ Absolute Counting Beads to each sample, so, by maintaining fixed the number of beads at 5000, we defined the volume of 5μL for analysis. In this way we were able to count EVs (**Figure 6C**).
Once set the experimental procedure, we compared the amount of EVs obtained by using the aforementioned methods of isolation. In our condition, we found ExoQuick™ solution to be the best EV isolation method in terms of reproducibility (**Figure 6D**), while the other methods showed great variability of the results obtained in the triplicated experiment. As regards the comparison between the EV production by the two osteosarcoma cell lines, only ExoQuick™ procedure led to isolate a comparable amount of vesicles, result confirmed at a later time by other methods (**Figure 9**).

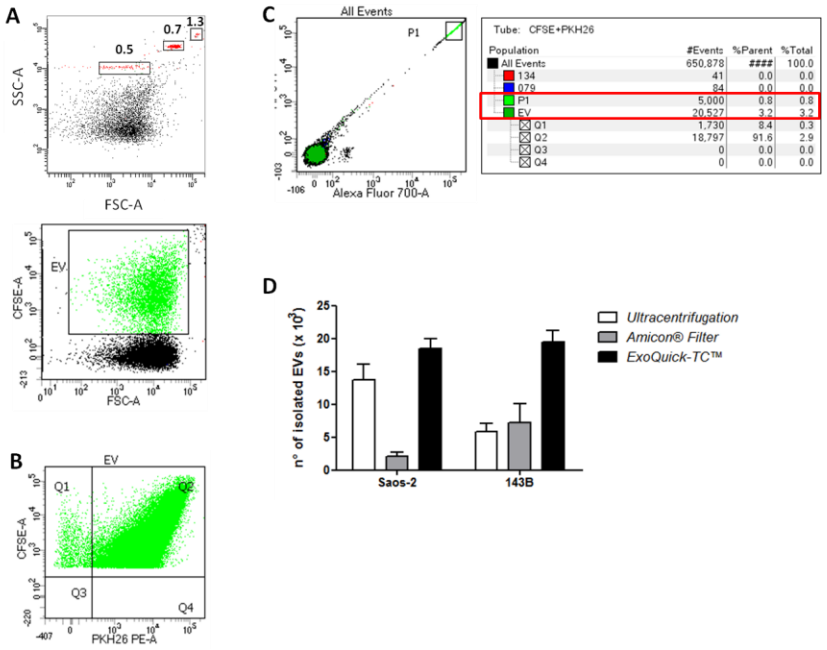

Figure 6. (A) Nanobeads dot-plot visualization used to create a gate of size <1µm for EVs. SSC, scattered light; FSC, forward-scattered light. **(B)** Dot-plot analysis showing purified $CFSE^{+}/PKH\text{-}26^{+}$ EVs by using fluorescence-activated cell sorting (FACS). (**C**) Dot-plot analysis showing CountBright Beads gate, indicated as P1 and representative table of EV count by maintaining fixed at 5000 the number of beads. **(D)** Dot-plot analysis showing EVs collected using the described methods.

In order to visualize EV release by the plasma membrane, we used three different osteosarcoma cancer cell lines: Saos-2, HOS and 143B, respectively low aggressive, non-metastatic and high metastatic cells. These cells were stained with rhodamine-coniugated phalloidin to detect F-actin. As reported by Antonyak and co-workers on breast cancer cells[91], also in our condition phalloidin staining revealed bubble-like structures on the surface of

osteosarcoma cells, resembling EVs about to be released (**Figure 7**).

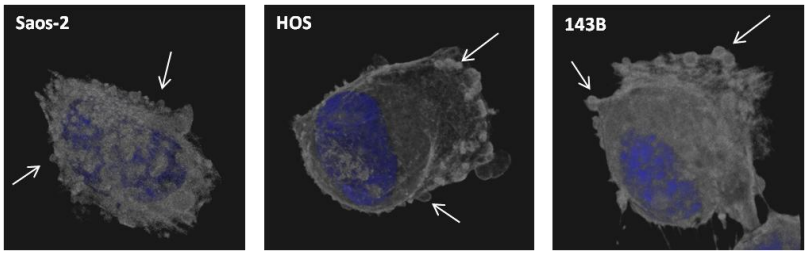

Figure 7. Confocal microscopy analysis of the indicated osteosarcoma cells stained with rhodamine-coniugated phalloidin (grey) and Hoechst (blue) to visualize EVs on plasma membrane (white arrows). Z-reconstructions are imported into LASX 3D Analysis (Leica Microsystems) software to obtain the three-dimensional surface rendering.

In order to confirm EV production by using a different method, we exploited CD63 expression, that is considered an EV marker[92,93]. As demonstrated by western blot analysis (**Figure 8A**), osteosarcoma-derived EVs express the CD63 marker, as also confirmed by FACS analysis assessing the PKH-26^{+}/CD63^{+} EVs (**Figure 8B**). Our results showed a comparable amount of both CD63 revealed by western blot and CD63^{+} percentage of EVs produced by osteosarcoma cell lines.

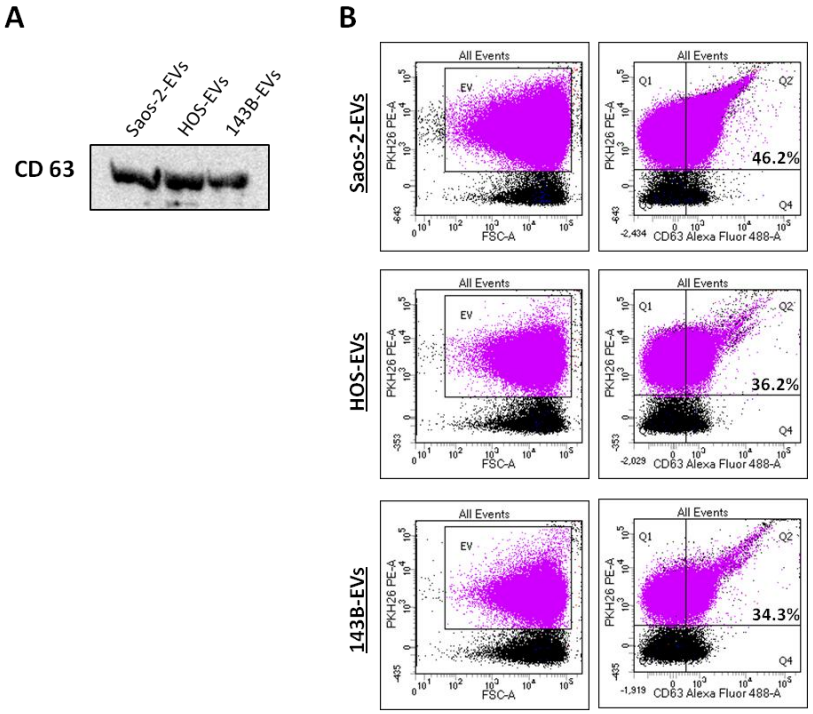

Figure 8. (A) WB analysis of CD63 in osteosarcoma-derived EVs. (B) Dot-plot analysis showing PKH-26^{+}/CD63^{+} EVs.

4.2 Osteosarcoma cell lines with different aggressiveness produce similar quantities of EVs.

We compared the amount of EVs produced by the different osteosarcoma cancer cell lines: Saos-2, HOS and 143B.Once isolated, EVs were quantified by using four different methods:

- CFSE^{+}/PKH-26^{+} EV quantification by FACS analysis
- EXOCET- quantification assay kit to assess the number of EVs,
- Tunable Resistive Pulse Sensing (TRPS) Technology by *Izon Science* to obtain the number of particles/ml,

- BCA assay for protein quantification.

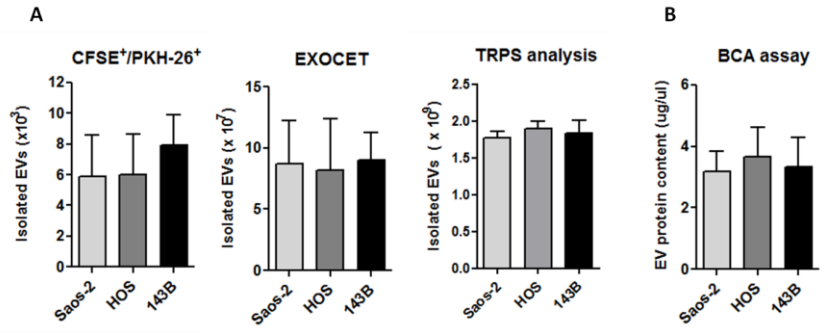

Figure 9. (A) Quantification of extracellular vesicles collected from 24 hour-conditioned media of the osteosarcoma cell lines by using the indicated methods. (B) Quantification of the EV protein content by BCA assay.

As shown in **Figure 9**, we demonstrate that these three cell lines, although with a different aggressiveness, produce comparable amount of EVs, unlike other cancer cells described in the literature. This unexpected result prompted us to study the EV's cargo to explore the possibility of a different mRNA or protein content conveyed in the EVs derived from the three osteosarcoma cell lines.

4.3 Effects mediated by osteosarcoma-derived EVs on normal NIH3T3 cells.

$CFSE^+/PKH\text{-}26^+$ EVs fuse into NIH3T3 target cells.

Starting from data in the literature concerning the capability of tumour-derived EVs to induce tumour phenotypes in normal cells[91], we investigated whether also osteosarcoma-derived EVs can be able to transform normal recipient cells. To this aim, we collected $CFSE^+/PKH\text{-}26^+$ EVs from Saos-2, HOS and 143B cells

as previously described and used them to treat NIH3T3 murine fibroblasts. $CFSE^+/PKH\text{-}26^+$ EVs isolated from osteosarcoma cell lines medium merged recipient fibroblasts, leading to $CFSE^+/PKH\text{-}26^+$ NIH3T3 cells, as assessed by fluorescent microscopy analysis (**Figure 10A**). EVs derived from different cell lines have the capability to fuse into target cells with a comparable effectiveness, as indicated by the percentage (about 80% of fusion) of $CFSE^+/PKH\text{-}26^+$ NIH3T3 cells shown in **Figure 10B**.

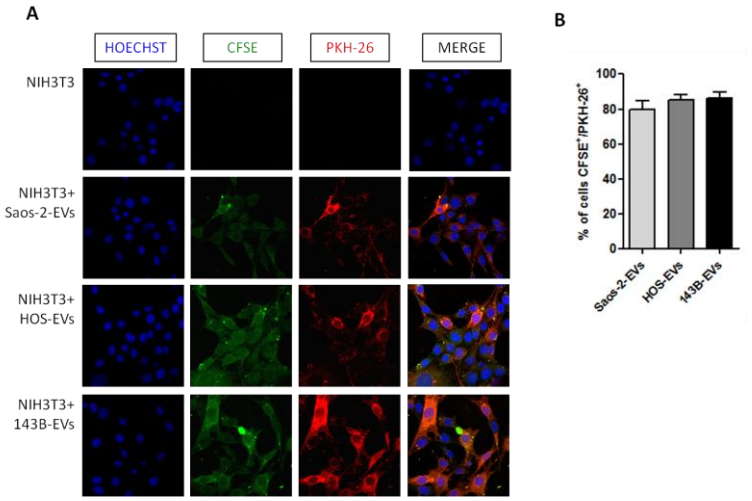

Figure 10: (A) Confocal microscopy analysis of NIH3T3 treated for 6 hours with $CFSE^+/PKH\text{-}26^+$ EVs. Pictures show the resulted $CFSE^+$ and $PKH\text{-}26^+$ recipient cells as proof of EVs fusion. (B) Quantification of $CFSE^+/PKH\text{-}26^+$ NIH3T3 cell percentage following the fusion with $CFSE^+/PKH\text{-}26^+$ EVs. Original magnification 60x.

These results were confirmed by FACS analysis performed on NIH3T3 treated for 6 hours with $CFSE^+/PKH\text{-}26^+$ osteosarcoma-derived EVs, as shown **Figure 11.**

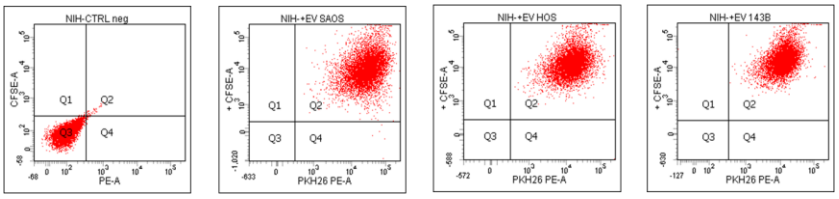

Figure 11. Dot-plot analysis of $CFSE^{+}/PKH\text{-}26^{+}$ NIH3T3 after fusion with $CFSE^{+}/PKH\text{-}26^{+}$ osteosarcoma-derived EVs.

Next, we used the aforementioned CD63 marker to monitor the fusion of tumour EVs into normal cells. To do this, we treated murine fibroblasts NIH3T3 for 72 hours with human osteosarcoma cell-derived EVs and then investigated the presence of human CD63 in the recipient murine fibroblasts. The specificity of anti-human CD63 antibody was confirmed by comparing the negative staining of untreated murine NIH3T3 cells to the 65% of CD63 positivity of untreated human fibroblasts. The FACS analysis confirmed the presence of human CD63 in treated NIH3T3, although with a variable efficiency of fusion, resulted at a higher percentages in the treatments with 143B-derived EVs (53.6%) than the treatments with the other cell line EVs (**Figure 12**).

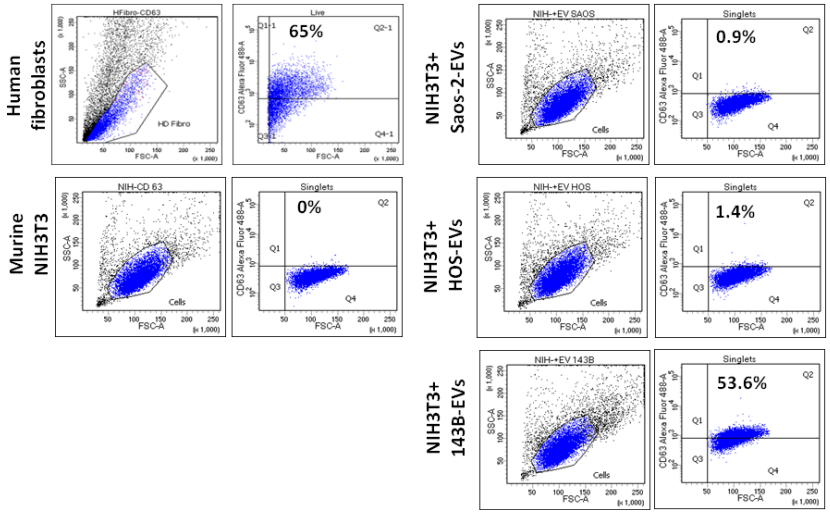

Figure 12. Dot-plot analysis of $CD63^+$ cells.

The treatment with osteosarcoma derived-EVs improves NIH3T3 proliferation and survival in low-serum conditions.

To investigate which kind of effect could be induced by the treatment of recipient normal cells with osteosarcoma derived-EVs, NIH3T3 cells were treated with a single shot of tumour-derived EVs and, after 72 hours, evaluated for proliferation by cell count. As shown in **Figure 13**, we obtained a statistically relevant result following the treatment with 143B derived-EVs.

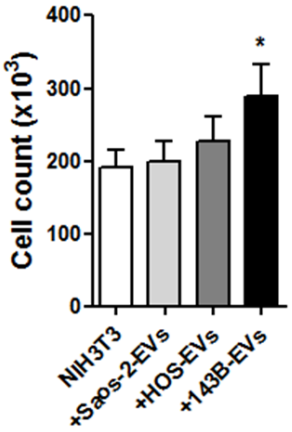

Figure 13. Cell count of NIH3T3 treated with osteosarcoma-EVs. *$p < 0.05$

Starting from this result on proliferation, we examined the effects of EV-mediated treatment on some of the most relevant signalling pathways involved in the regulation of cell proliferation. We performed western blot analysis for activated AKT and ERK proteins in NIH3T3 treated with osteosarcoma-derived EVs. As shown in **Figure 14**, an increased expression of phospho-AKT and phospho-ERK was found, especially in the treatment with HOS- and 143B-derived EVs.

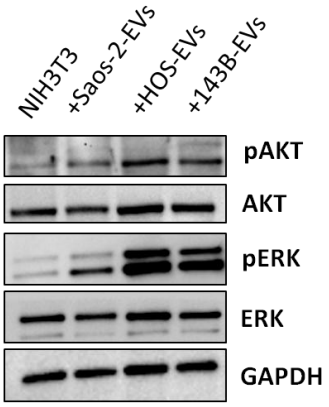

Figure 14. Representative Western blot analysis of phosphorylated AKT (pAKT), total AKT, phosphorylated ERK (pERK) and total ERK in NIH3T3 treated with osteosarcoma-derived EVs, normalized versus housekeeping GAPDH. Untreated NIH3T3 were used as control.

To further investigate the effects mediated by tumoral EV treatment on NIH3T3, we performed experiments in starvation conditions which, in the long run, are known to reduce proliferation (2% FBS condition) or induce cell death (BSA condition) in normal fibroblasts. As shown in **Figure 15**, the treatment of starved NIH3T3 with osteosarcoma derived-EVs for 72h induced an increase of cell count, highlighting the capability of tumoral EVs to induce survival in NIH3T3 that, usually, are not able to survive in low serum conditions.

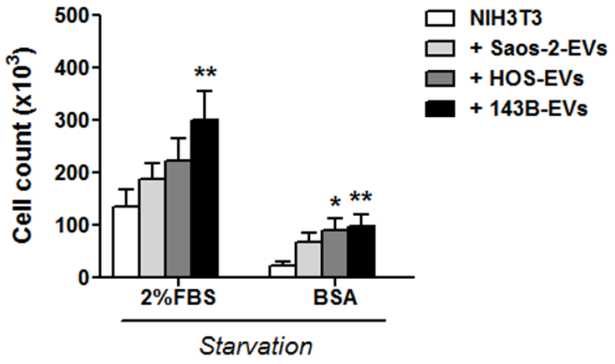

Figure 15. Cell count of NIH3T3 treated with osteosarcoma derived-EVs in starvation conditions. * p <0.05, ** p <0.01 versus the relative control.

Moreover, to better understand these effects on NIH3T3 survival, we evaluated the percentage of apoptotic fibroblasts after the EV-treatment in BSA condition, by using Annexin V assay. As reported in **Figure 16**, the percentage of live NIH3T3 cells increased after the treatment with osteosarcoma-derived EVs from 76% in control BSA condition to 91-93% in treated cells, while the percentage of apoptotic fibroblasts drastically decreased, showing a behaviour comparable to NIH3T3 cultured in canonical condition (10% FBS). Beside the analysis of apoptosis pattern, we studied the cell cycle rate in starvation condition, finding an increased of NIH3T3 in G0/G1 phase following EV treatment (**Figure 17**), thereby indicating that the treatment with osteosarcoma-derived EVs maintained NIH3T3 alive, but blocked in G0/G1 stage.

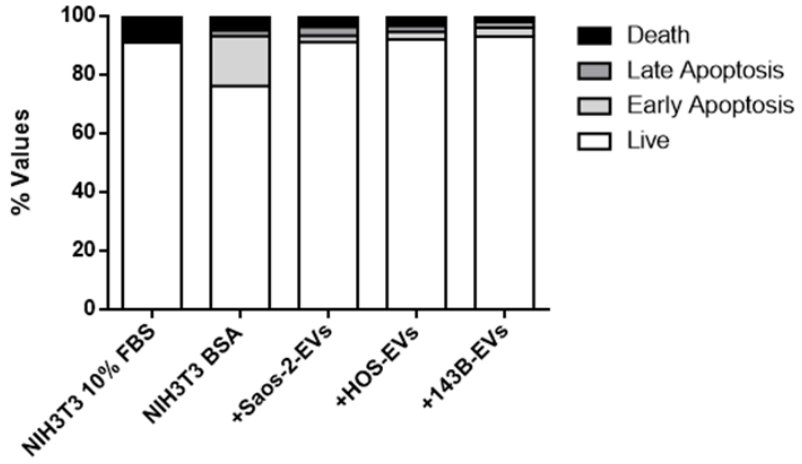

Figure 16. Annexin V assay analysis of NIH3T3 treated with osteosarcoma-derived EVs in BSA condition, compared to canonical culture condition (10% FBS).

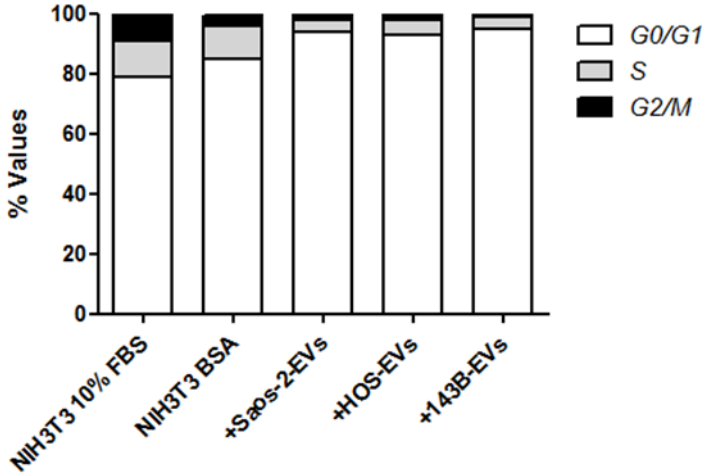

Figure 17. Cell cycle analysis of NIH3T3 treated with osteosarcoma-derived EVs in BSA condition, compared to canonical culture condition (10% FBS).

To exclude the possibility of any aspecific effect mediated by extracellular vesicles, and in order to confirm the transforming power of osteosarcoma derived-EVs, we performed the same kind of experiments by using EVs isolated from normal cells, as NIH3T3, human Mesenchymal Stromal Cells (MSC) and human osteoblasts (HOB). After the treatment, NIH3T3 showed no difference in terms of proliferation or survival in comparison to controls (**Figure 18**).

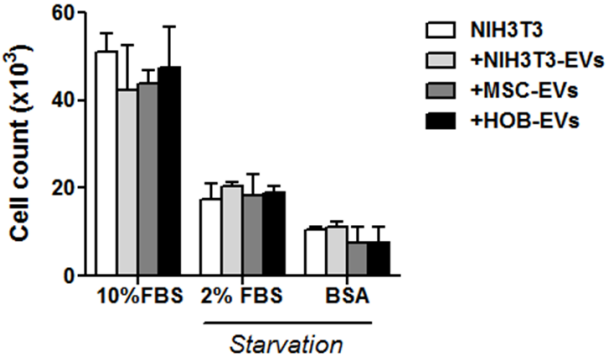

Figure 18. Cell count of NIH3T3 treated with EVs derived from normal cells.

NIH3T3 treated with osteosarcoma-derived EVs exhibited enhanced migration capability and an acquired anchorage-independent growth.

To gain insight into the involvement of osteosarcoma-derived EVs in the tumour-like transformation of normal cells, we assessed the capability of EV-treated NIH3T3 cells to migrate and to grow in anchorage-independent condition. To this aim, NIH3T3 cells were treated with tumoral EVs for 5 hours and then evaluated for their migration capability by wound healing assay, showing a higher area covered by cells if compared to the control, as indicated by the reduction of the wound size (**Figure 19**). Moreover, we exploited the inability of control NIH3T3 fibroblasts to form colonies in soft

agar to demonstrate that the treatment with osteosarcoma-derived EVs induced on these cells the acquired capability to grow under anchorage-independent conditions **(Figure 20**). Thus, the EV-mediated transfer of cancer cell material to normal cells is indeed capable of endowing normal cells with the features of tumorigenic transformation.

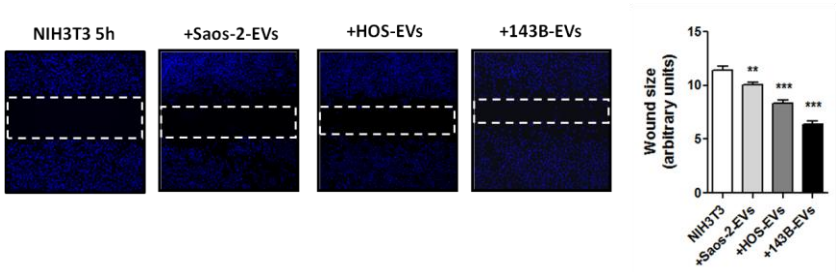

Figure 19. Representative pictures and the relative quantification graph of the wound size in a wound healing assay performed on NIH3T3 treated with osteosarcoma-derived EVs. Original magnification 20x.
***p* <0.01, **** p* <0.0001

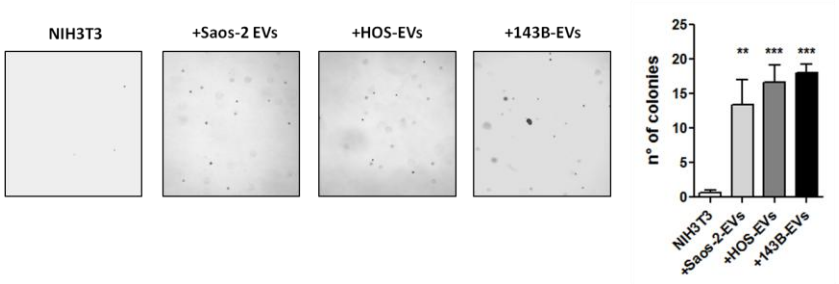

Figure 20. Representative images and quantitative analysis of colony formation in the anchorage-independent growth assay. Original magnification 10x.
***p* <0.01, **** p* <0.0001

Osteosarcoma-derived EVs transfer osteogenic and tumour markers into recipient NIH3T3 cells.

To better define the effects of tumour-derived EVs, we studied the capability of EVs to transport their mRNA content into recipient cells. In our system we used human osteosarcoma-derived EVs to treat murine normal fibroblasts allowing us to analyse the presence of human mRNA in murine fibroblasts. Moreover, given that osteosarcoma arises from transformed cells of the osteoblastic lineage, we evaluated the expression of osteoblastic and tumorigenic mRNA. As reported in **Figure 21**, following the treatment with EVs, murine NIH3T3 expressed human and murine ALkalin Phosphatase (ALP) mRNA, a specific marker of osteoblastic differentiation as well as the murine isoform of matrix metallopeptidase 9 (MMP-9) and the human isoform of tumor necrosis factor-α (TNF-α), well known markers of tumorigenesis.

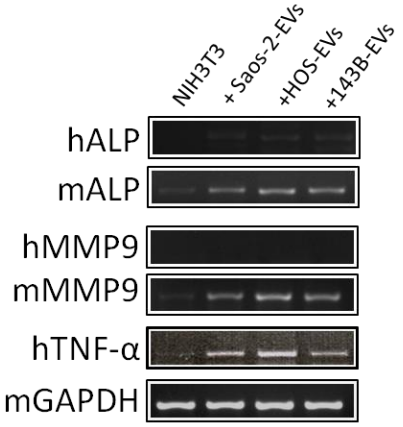

Figure 21. mRNA expression in NIH3T3 treated with osteosarcoma-derived EVs.

4.4 Effects of osteosarcoma-derived EVs on normal human bone cells.

Basing on the tumoral transformation resulted by treating NIH3T3 fibroblast with osteosarcoma-derived EVs, we decided to study the effects of osteosarcoma-derived EVs on bone cells.
To this aim, we performed experiments using these extracellular vesicles to treat the bone microenvironment cells: mesenchymal stromal cells (as osteoblast progenitors), primary human osteoblasts and monocytes (as osteoclast precursors).

Effects of osteosarcoma-derived EVs in Mesenchymal Stromal Cells (MSCs).

We collected osteosarcoma-derived EVs as previously described and used them to treat healthy donor-derived MSCs. Twenty-four hour treatment induced no differences in proliferation, assessed by cell count (**Figure 22**).

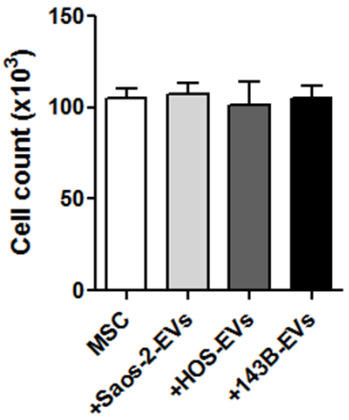

Figure 22. Cell count of MSCs treated for 24h with the indicated osteosarcoma-derived EVs.

To study more in detail this effect, we treated MSCs with osteosarcoma-derived EVs for 3 weeks and then assessed their positivity for osteoblast markers. Despite the absence of osteogenic medium, indispensable to trigger osteoblastic differentiation, we surprisingly found a slight induction of ALP following the treatment with Saos2-derived EVs, as well as a relevant induction of mineralization assessed by Alizarin Red staining, especially following the treatment with Saos2- and HOS-derived EVs (**Figure 23**).
In order to verify whether this effect could be enhanced by the induction of osteoblastic differentiation, we treated MSCs with osteogenic medium and with osteosarcoma-derived EVs. To avoid the achievement of a plateau condition, this experiment lasted 10 days, instead of the canonical 21 days of treatment in osteogenic medium. At the end of this experiment, we found once again both an increase of ALP and a massive induction of mineralized noduli stained by Alizarin Red in Saos2-derived EV treatment (**Figure 24**).

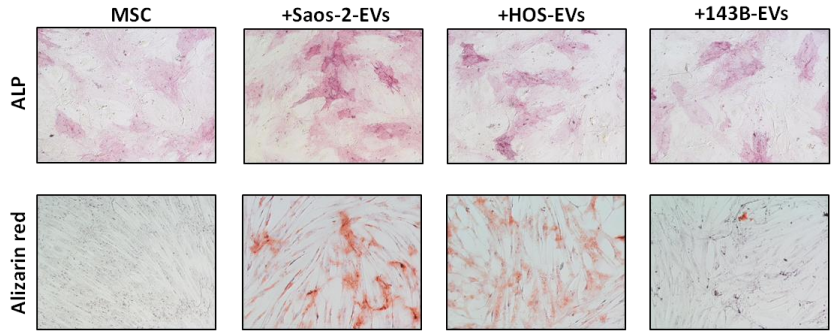

Figure 23. Representative pictures of ALkaline Phosphatase (ALP) and Alizarin red staining of MSCs treated for 3 weeks with medium supplemented with 10% FBS and the indicated osteosarcoma-derived EVs. Original magnification 20x.

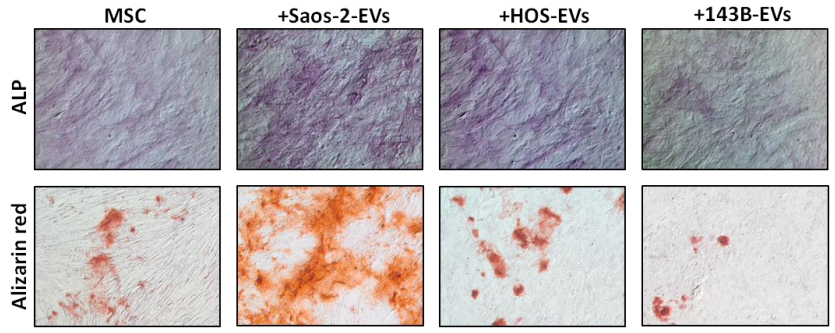

Figure 24. Representative pictures of ALkaline Phosphatase (ALP) and Alizarin red staining of MSCs treated for 10 days with osteogenic medium and the indicated osteosarcoma-derived EVs. Original magnification 20x.

Effects of osteosarcoma-derived EVs on human osteoblasts (hOBs).

As regards osteoblast cells, we performed the same experiments described above, by treating human primary osteoblasts with osteosarcoma-derived EVs. After 24h of treatment, hOBs showed not relevant modulation in proliferation and differentiation (**Figure 25**).

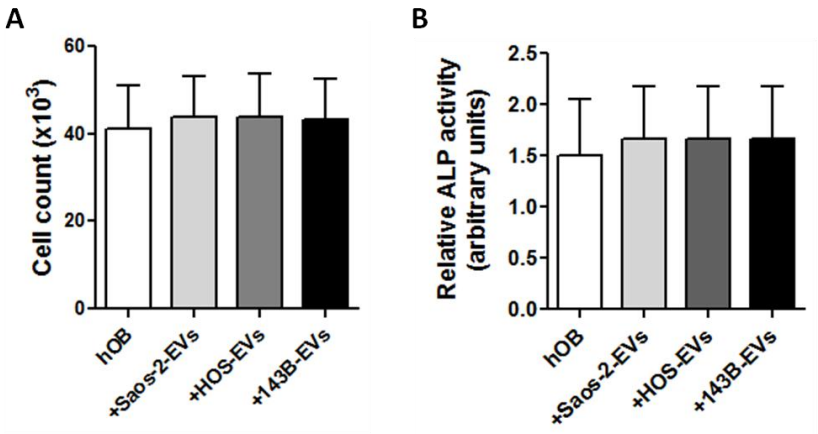

Figure 25. (A) Cell count of osteoblasts treated for 24h with the indicated osteosarcoma-derived EVs. (B) Quantification of hOB treated for 72 hours with medium supplemented with 10% FBS and the indicated osteosarcoma-derived EVs

Moreover, in order to further investigate the ability of the tumour-EVs to transform normal cells, we evaluated tumour-like phenotypes in EV-treated osteoblasts. To this aim, as described for NIH3T3 cells, normal osteoblasts were treated with osteosarcoma-derived EVs for 5 hours and then evaluated for their capability to migrate by a wound healing assay. Our results showed a significantly improved migration demonstrated by the reduction of the wound size **(Figure 26**). Next, we investigated the anchorage-independent growth of EV-treated osteoblasts finding, also in this condition, an acquired capability to form colonies in soft agar (**Figure 27**).

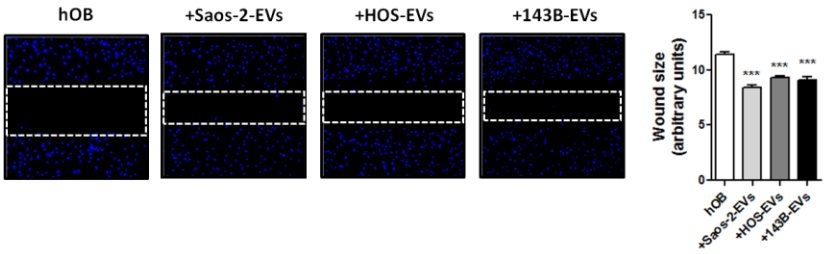

Figure 26. Representative pictures and the relative quantification graph of the wound size in a wound healing assay performed on hOB treated with osteosarcoma-derived EVs. Original magnification 20x. *** p <0.0001

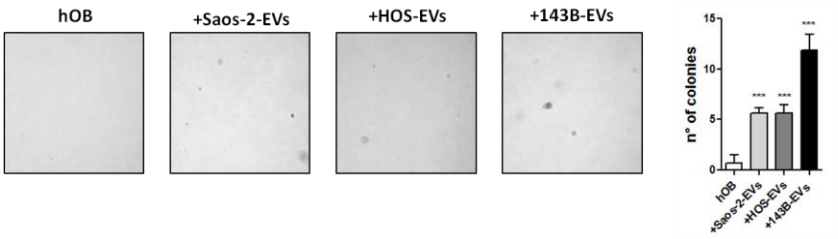

Figure 27. Representative images and quantitative analysis of colony formation in the anchorage-independent growth assay. Original magnification 10x.
**p <0.01, *** p <0.0001

Finally, in order to investigate the effects caused by osteosarcoma-derived EVs on hOBs, we analysed the transcriptional levels of osteoblast differentiation markers, such as ALP, COLL1A2 and RUNX2, as well as genes involved in the tumourigenic transformation, as TNF-α, TGF-β and IL6. As shown in **Figure 28**, our findings evidenced that in particular RUNX2 and TNF-α mRNA were increased in osteoblasts treated with osteosarcoma-derived EVs.

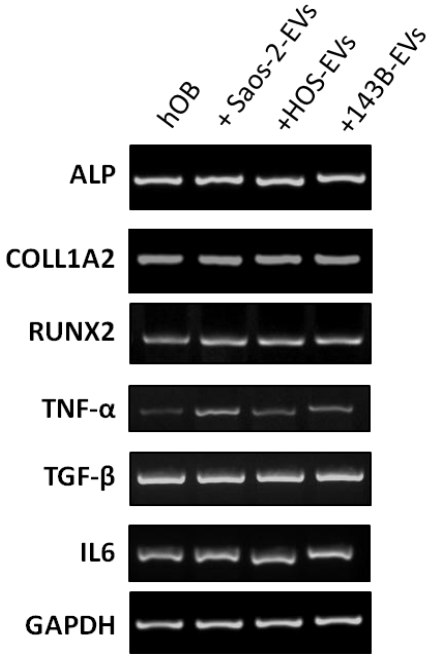

Figure 28. mRNA expression levels in human osteoblasts treated with osteosarcoma-derived EVs.

Effects of osteosarcoma-derived EVs on human monocytes.

As regarding the osteoclast precursors, we treated healthy donor-derived monocytes with canonical MCSF (20ng/ml) as control condition of proliferation and with osteosarcoma-derived EVs for 24 hours. **Figure 29** highlighted a significant increase in monocyte proliferation treated with HOS-derived EVs compared to control.

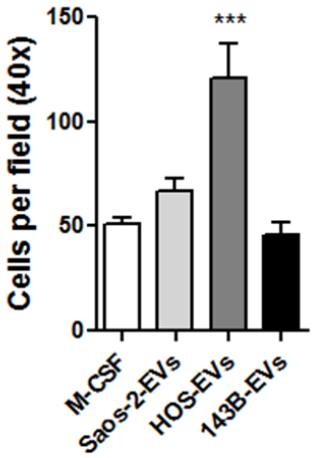

Figure 29. Cell count of monocytes treated for 24h with MCSF (ctl) or with indicated osteosarcoma-derived EVs. *** p <0.0001

Next, in order to assess any effect on osteoclastogenesis, we treated healthy donor-derived monocytes for 2 weeks with the canonical M-CSF (20ng/ml) and RANKL (30ng/ml) treatment as control condition and with osteosarcoma-derived EVs. As shown in **Figure 30**, osteosarcoma-derived EV alone resulted able to induce the formation of $TRAP^+$ multinucleated osteoclasts, although in a lower amount than canonical treatment.

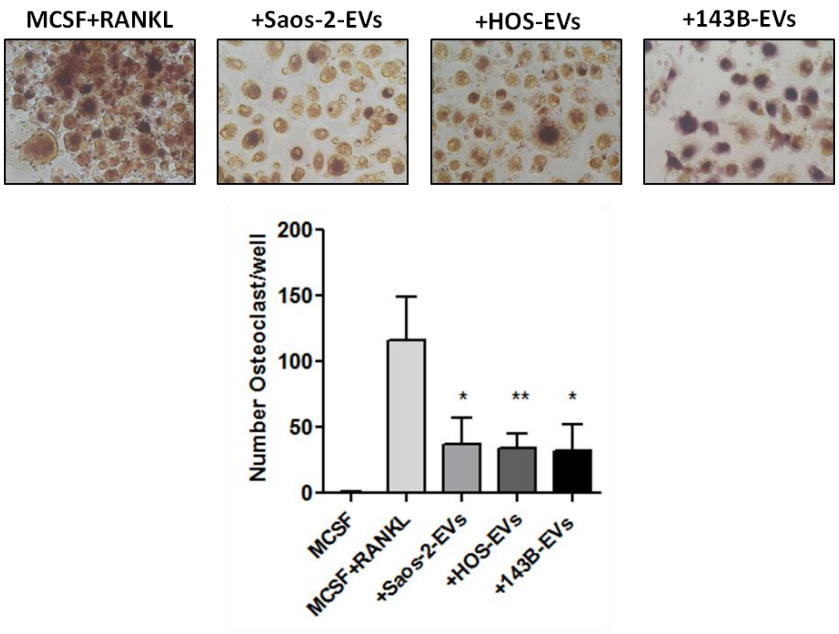

Figure 30. Representative pictures of TRAP staining (upper panels) and the relative count (lower panel) of $TRAP^+$ Osteoclasts obtained by treating monocytes with canonical treatment (MCSF+RANKL) or with the indicated osteosarcoma-derived EVs. Original magnification 20x.
* vs MCSF. * $p<0.05$, ** $p<0.01$.

In order to explain the induction of monocyte proliferation and differentiation observed following EV treatments, we assessed the presence of osteoclast-stimulating factors (RANK, RANKL and M-CSF) in osteosarcoma cell lines and derived EVs, by FACS analysis.
All cell lines expressed high levels of these cytokines, in particular the high metastatic 143B cells. As regarding the corresponding EVs, we found them positive for RANK and RANKL, in particular HOS- and 143B-derived vesicles. Only HOS-derived EVs showed high M-CSF expression level (**Figures 31-32**).

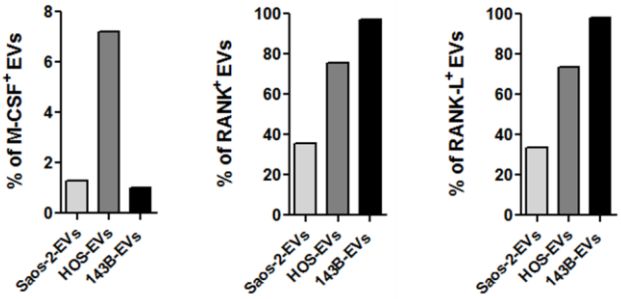

Figure 31. Analysis of $MCSF^{+}$/$RANK^{+}$/$RANKL^{+}$ EVs percentage.

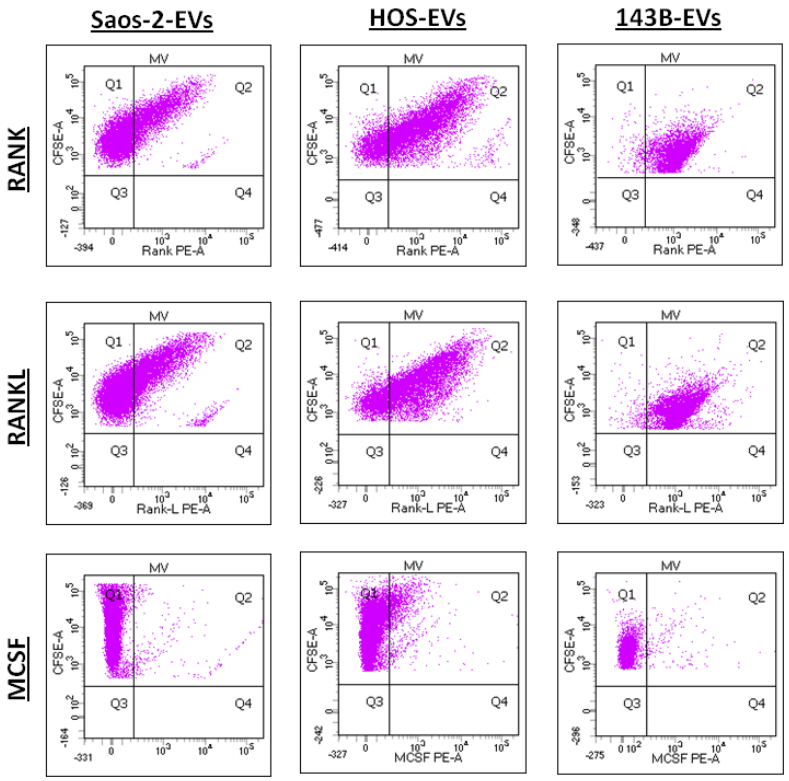

Figure 32. Dot-plots analysis showing RANK/RANKL/MCSF expression in osteosarcoma-derived EVs.

4.5 To use EVs as prognostic/diagnostic markers.

Once demonstrated some features of this new type of cell communication mediated by EVs, we focused our attention on the feasibility to use these vesicles as prognostic markers in osteosarcoma.
GD2 ganglioside is a well known marker of neuroblastoma[94,95], it has been described as a component of neuroblastoma-derived EV cargo[96] and in a recent study it was reported that GD2 was stably expressed in osteosarcoma cells[97].
So we studied the expression of surface protein GD2 ganglioside in our nanoparticles. To this aim, we performed a cytofluorimetric assay on osteosarcoma cell lines and their derived EVs by using anti-human GD2-PE antibody. As reported in **Figure 33**, osteosarcoma cell lines with increasing aggressiveness expressed increasing levels of GD2 on their surface, and the same result was also obtained when we analyzed osteosarcoma-derived EVs.

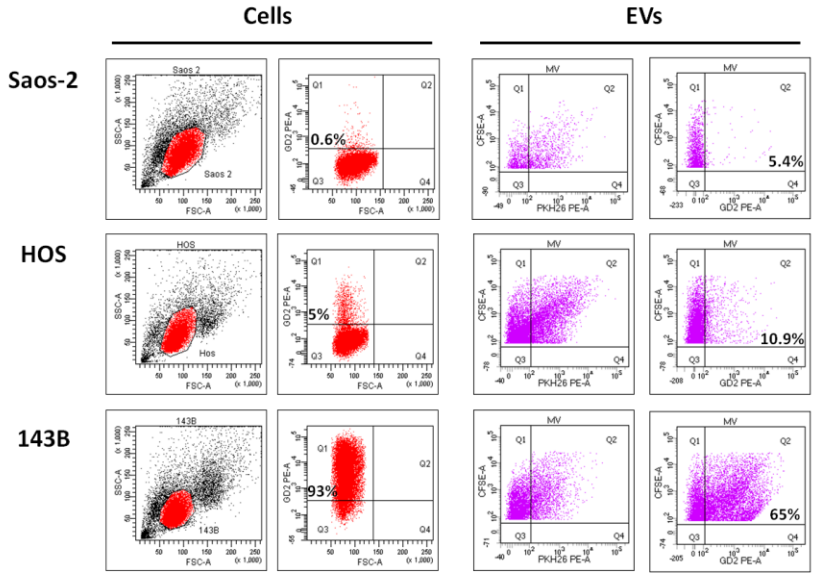

Figure 33. Dot-plot analysis showing $GD2^+$ osteosarcoma cell lines (left panel) and $GD2^+$ osteosarcoma-derived EVs (right panel).

4.6 To inhibit EV production in osteosarcoma cells.

We investigated the capability to counteract EV production by acting on remodelling of actin cytoskeleton. In particular, we focused our attention on Y-27632, an inhibitor of Rho-associated coiled–coil containing protein kinase (ROCK). To test the reduction of EV production as consequence of Y-27632 treatment, we evaluated the amount of EV by using EXOCET method, as described before. In **Figure 34** is shown that Y-27632 treatment was able to reduce significantly the amount of osteosarcoma EVs and in particular the major effect was obtained in HOS cell lines.

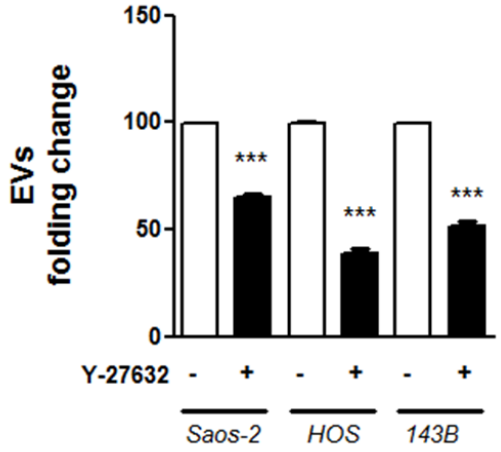

Figure 34. EXOCET quantification of osteosarcoma-derived EVs with or without the treatment with Y-27632. *** p <0.0001

5. Discussion

Osteosarcoma is the most common primary malignant bone tumour in children and adolescents. With one of the lowest survival rates among paediatric cancers, Osteosarcoma imparts a 5-year survivorship of 70% in patients treated for localized disease, but only 30% when metastases are present. Therefore, there is a critical need to better understand the underlying mechanisms of disease development and progression.

Cell can communicate with neighbouring cells or with distant cells through the secretion of extracellular vesicles (EVs). The release of EVs from different types of high-grade or aggressive forms of human cancer cells into their surroundings is becoming increasingly recognized as a feature of tumour biology[96,98,99].

Hence, as the first aim of this study, we pointed to investigate the ability of human osteosarcoma cell lines to produce EVs. The isolation of EVs is a crucial point for researcher that study this topic because there is a great variety of methods and each presents some limitations. Moreover, high sensitive equipment is needed to work with EVs, because of their very little size. Therefore, taking into consideration these issues, the first part of this study has been spent to define the best methods for EV isolation and visualization in dependence on our experimental conditions. First of all, we compared 3 of the most used methods to isolate EVs: the ultracentrifuge, Amicon filters and the ExoQuick™ polymer.

In order to compare the amount of EVs isolated by each method, we needed to visualize and, if possible, to count these particles by fluorescence-activated cell sorting (FACS) analysis. Since this instrument is routinely used to analyse cells, we adapted our FACS protocol by introducing the following expedients:

1) fluorescence dyes: we used CFSE and PKH-26 dyes to stain osteosarcoma cells, and obtain $CFSE^{+}/PKH\text{-}26^{+}$ EVs in the conditioned media. In this way, we were able to discriminate fluorescent EVs from background noise by FACS analysis.

2) beads with known size: by using 0.5, 0.7 and 1.3 µm beads, we were able to define the gate in which we expected to find fluorescent EVs by FACS analysis.
3) CountBright beads: by adding these beads to each sample, we knew exactly the volume analysed in each condition, allowing us to define the concentration of EVs by FACS analysis.
Once set this procedure, we compared the amount of EVs produced by 2 osteosarcoma cell lines and isolated by using ultracentrifuge, Amicon filters and the ExoQuick™. Our results prompted us to choose ExoQuick™ as unique isolation method for conducting our experimental project. Indeed, we demonstrated that this polymer guaranteed not only the higher amount of isolated vesicles, but also the best reproducible results.
Once verified that osteosarcoma cells produce EVs, the second step was to obtain EV visualization and, at the same time, to quantify them. Basing on Antonyak et al. work, we exploited phalloidin staining to unveil EVs on the plasma membrane of osteosarcoma cells. By three-dimensional reconstruction of confocal microscopy z-stack series, we demonstrated that osteosarcoma cells produced EVs and, as expected, their release occurred at the apical portion of the plasma.
Next, we intended to compare EV production of three osteosarcoma cell lines with increasing aggressiveness. Indeed, as reported for other types of cancers, we expected to find a correlation between osteosarcoma aggressiveness and the amount of produced EVs. As regards EV quantification, once again we had to deal with the different methods and protocols described in the literature. First of all, we assessed the expression of CD63, a specific EV marker, in osteosarcoma EVs, by FACS analysis, and in their protein lysates, by western blot. Our results suggest that, in our experimental conditions, CD63 analysis of osteosarcoma-derived EVs is not a useful tool, because of the incomplete staining of EV population, obtained by PKH-26 dye. Indeed, less than 50% of total EVs resulted $CD63^{+}$, prompting us to identify other methods to quantify tumoral EVs.

To this aim, we compared EV production by using other methods well known in literature, as the count of $CFSE^+/PKH\text{-}26^+$ EVs by FACS analysis, EXOCET quantification assay, the TRPS analysis and the quantification of total proteins conveyed by EVs. By using these methods we ascertained that the amount of total EV produced by each osteosarcoma cell line was comparable, unlike our expectations. Moreover, the TRPS analysis performed by *Izon Science* attested the range sizes of our osteosarcoma nanoparticles at 50-200nm, confirming their nature of EVs.
In order to further characterize EVs, we assessed the effects of tumoral EVs on recipient cells. Generally, tumour cells may alter the surrounding stroma inducing cell modification and, recently, it has been also described for other tumour cells the capability of their EVs to induce transformation in target cells[91]. We chose a murine fibroblast cell line, NIH3T3, as recipient cells to study the tumoral effects of osteosarcoma-derived EVs in a context different from the bone tissue in which this tumour develops. We obtained the first evidence of the osteosarcoma-derived EV capability to fuse into target cells by observing $CFSE^+/PKH\text{-}26^+$ NIH3T3 after the treatment with $CFSE^+/PKH\text{-}26^+$ EVs, as assessed by both confocal microscopy and FACS analysis. Moreover, although the inadequate result obtained with CD63 staining as quantification tool, we exploited human $CD63^+$ EVs produced by osteosarcoma cells to investigate their fusion on mouse target cells, thereby evaluating the transfer of human material from osteosarcoma cells to murine fibroblast NIH3T3. To test this hypothesis, we treated murine NIH3T3 cells with osteosarcoma-derived EVs and then assessed the presence of human CD63 by FACS analysis. Although the production of $CD63^+$ vesicles has resulted comparable among the three cell lines, we observed a variable efficiency of fusion, resulted at the highest percentages in the treatments with 143B-derived EVs, demonstrating that this high metastatic osteosarcoma cell line produced EVs able to fuse in to target cells more efficiently than less aggressive cell lines HOS and Saos-2. Moreover, this finding suggests that the pattern of effects

mediated by these vesicles cannot be referred in general terms to "osteosarcoma" cells, but reflects the specific features of the cell of origin.
Next, we evaluated transformation towards tumoral-like phenotype in EV-treated NIH3T3. To this aim, as a proof of concept of the transforming power of these vesicles, we decided to apply an acute stimulation, considering just one treatment with osteosarcoma-derived EVs. By using canonical culture condition (medium supplemented with 10% FBS), the treatment of NIH3T3 with osteosarcoma-derived EVs showed an increase in their proliferation and in the activation of key pathways involved in cell proliferation, especially following the treatment with 143B-derived EVs. This result once again indicates a differential pattern of effects mediated by EVs deriving from different osteosarcoma cell lines, in particular related to their aggressiveness. When we cultured normal NIH3T3 in low-serum condition (medium supplemented with 2% FBS) or starvation condition (medium supplemented with 0.25% BSA), we found as expected a decrease of proliferation and an induction of apoptosis, respectively. Surprisingly, the treatment with osteosarcoma-derived EVs rescued fibroblast capability to survive in both types of media. In particular, in BSA condition, we counted a higher number of NIH3T3 that, as demonstrated with Annexin V assay and cell cycle analysis, resulted to be Annexin negative and blocked in G0/G1 phase. So, after the treatment with osteosarcoma-derived EVs NIH3T3 were alive and survivor, although not proliferating, despite the starvation condition. To confirm this finding and exclude the possibility of any aspecific effect, we treated NIH3T3 with EVs isolated from normal cells, as NIH3T3 themselves, human Mesenchymal Stromal Cells (MSC) and human osteoblasts (HOB). Indeed, we found no changes in proliferation rate of NIH3T3 so treated.
Basing on these results, we decided to study other features regarding the tumoral transformation of normal NIH3T3. Interestingly, osteosarcoma-derived EVs have been demonstrated

to induce in recipient NIH3T3 an increase of migration and the acquired capability to growth in an anchorage-independent manner. Also in these conditions, we found that greater effects were induced by 143B-derived EVs, confirming that the signals conveyed by these tumoral vesicles reflect specific features of the cell of origin, which are known to have a high migration rate.
Moreover, since our preliminary evidence suggested the carriage of human material in murine fibroblasts, as described before, we analysed the expression of human and murine osteoblastic and tumorigenic mRNAs in NIH3T3 after the EV treatment. Murine NIH3T3 expressed human and murine ALkalin Phosphatase (ALP) mRNA, a specific marker of osteoblastic differentiation and, at the same time, these cells expressed murine isoform of matrix metallopeptidase 9 (MMP-9) and the human isoform of tumor necrosis factor-α (TNF-α), that are well known markers of tumorigenesis. The presence of human mRNA in murine fibroblasts confirmed the ability of tumoral EVs to transfer material of cell of origin (exogenous). But, more intriguing, the endogenous expression of markers of osteoblastic lineage or tumoral cells suggests that osteosarcoma-derived EVs convey within them some transcription factors or upstream signals able to induce the transcription of those specific markers. Taken together, these findings strongly support the great transforming power that these particles have.
These data prompted us to study the effects mediated by osteosarcoma-derived EVs on cells of the bone microenvironment, in which the tumour develops and likely establishes a crosstalk with resident cells. It is known that osteosarcoma can form both osteoblastic and osteolytic lesions, due to an increase of osteoblastic and osteoclastic activity, respectively. So, to this aim, we assessed the effect of tumoral vesicles on human osteoblasts (hOBs), Mesenchymal Stromal Cells (MSC) as osteoblast precursors, and human healthy-donor monocytes, as osteoclasts precursors. Our results on MSC showed that the treatment with osteosarcoma-derived EVs in normal culture conditions did not

affect the proliferation, but induced a slight increased in differentiation, as demonstrated by the presence of ALP^+ and Alizarin red^+ MSCs following Saos-2-derived EVs. These results prompted us to evaluate EV-treatment effects upon the induction of osteogenic differentiation. Indeed, MSCs, treated with osteogenic medium for 10 days, despite the canonical 3 week-treatment, and with tumoral EVs showed a higher differentiation toward the osteoblastic lineage, becoming ALP^+ as well as Alizarin Red^+ especially in Saos2-derived EV treatment, compared to the control. In order to avoid a plateau effect due to the canonical treatment with the osteogenic medium, we chose to reduce the duration of the protocol to better appreciate any effect mediated by EV treatment.

These findings suggest that osteosarcoma cancer cells producing EVs in the bone microenvironment induce the differentiation of osteoblast precursors, likely leading to the formation of aberrant tumoral bone matrix.

As regarding the effects on differentiated osteoblasts, following the treatment with osteosarcoma-derived EVs, they showed no modulation in proliferation and differentiation, being comparable to the control condition, but they showed an increased capability to migrate and to form colonies in soft agar, therefore acquiring typical features of tumour cells. For these reasons, we investigated the expression of osteoblastic and tumorigenic markers in EV-treated hOBs. Among mRNAs studied, we highlighted the enhanced expression of RUNX2 and TNF-α in hOBs that received osteosarcoma-derived EVs. The correlation between high expression of RUNX2 and the oncogenesis of bone tumours as well as bone metastases has been already described[100] thus strengthening our hypothesis of EV involvement in the vicious cycle established between osteosarcoma and bone cells.

As regards osteoclasts and osteoclast precursors response to EV treatments, we found a great induction of proliferation following HOS-derived EV treatment of monocytes, as well as the formation of $TRAP^+$ multinucleated cells after two weeks of treatment,

although in a lower amount than canonical treatment (M-CSF and RANKL). Since we obtained this finding by treating monocytes with only osteosarcoma-derived EVs and without pro-osteoclastogenic cytokines, the presence of $TRAP^+$ multinucleated osteoclasts, although in a low amount, represents a first evidence of EV capability to support, alone, osteoclastogenesis. Indeed, by FACS analysis we confirmed the presence of MCSF, RANK and RANKL in EVs derived from all 3 type of osteosarcoma cell lines, although in different quantities. Therefore, analysing these data, we can conclude that osteosarcoma EVs are able to alter the balance of bone homeostasis and to induce non-canonical differentiation and tumorigenic mechanisms in normal cells, that can be associated to osteosarcoma oncogenesis.

Once demonstrated the crucial role of these nanoparticles in tumour cell communication, we tried to exploit this mechanism by using EVs as prognostic marker. GD2 ganglioside is a well known marker for detection of neuroblastoma[101,102] and is expressed also in osteosarcoma patients[97]. Hence, we demonstrated that EVs derived from osteosarcoma cell lines with increasing aggressiveness showed increasing expression of GD2 marker. This finding can be useful in the prognostic and diagnostic approaches to osteosarcoma, in particular considering that EVs can be very easily detected and isolated from the bloodstream and other biological fluids.

Finally, considering the transforming power of osteosarcoma EVs, we studied the possibility to inhibit the extracellular secretion of these vesicles.

Starting from data in the literature showing the suppression of osteosarcoma by the inhibition of ROCK signalling and the role of GTPase RhoA to trigger a specific signalling pathway essential for microvesicles biogenesis[103,104], we evaluated the effects of cytoskeleton remodeling on the EV production in osteosarcoma cell lines treated with the protein kinase ROCK inhibitor, Y-27632. This treatment reduced the amount of EVs produced by tumour cells, thereby strengthening the feasibility to use this drug in the

therapeutic approach to osteosarcoma patients and further underlining the involvement of EV signalling in oncogenesis.
Our work highlights the relevance of EV shedding by osteosarcoma cells as a crucial process exploited by tumour to alter the microenvironment in which it arises. In this context, we demonstrated that tumoral EVs may be involved in cancer onset and progression, especially by transforming normal cells of the tumour microenvironment. This effect would be consistent with the idea that the expansion of a tumour mass would not necessarily depend solely on the proliferation of the cancer cells but rather could include as well the aberrant growth of normal cells exposed to tumour-derived EVs. Should this notion turns out to be true, the scientific community needs to adjust the common understanding of cancer progression *in vivo*, by including the potential contribution of EVs.

6. Materials & Methods

6.1 Cell culture

The human osteosarcoma cell lines and NIH3T3 were purchased from ATCC.
Primary human femoral osteoblasts and primary human fibroblasts were purchased from ScienCell™.
Isolation of mononuclear cells and *ex vivo* expansion of MSCs were performed from healthy donors who donate bone marrow cells for transplantation at the Bambino Gesù Children's Hospital, as described in Bernardo et al. work[105]. Briefly, mononuclear cells were obtained from bone marrow aspirates of HDs by density gradient centrifugation (Ficoll 1.077 g/ml; Lympholyte, Cedarlane Laboratories Ltd.) and plated in noncoated 75-175 cm^2 tissue culture flasks (BD Falcon) at a density of 160.000/cm^2 in complete culture medium: DMEM (Eurocloney) supplemented with 10% fetal bovine serum (FBS, Gibco), 100 units/ml penicillin/ streptomycin (Euroclone) and 2mM L-glutamine (Euroclone). Cultures were maintained at 37°C in a humidified atmosphere, containing 5% CO_2. After 48 hours in adhesion, non-adherent cells were removed and culture medium was replaced twice a week. MSCs were harvested, after reaching about 80% confluence, using Trypsin (Euroclone), and they were propagate at 4.000 cells/cm^2
All cell lines were grown in Dulbecco's modified Eagle's medium (DMEM) (Euroclone) supplemented with 10% FBS, 100 units/ml penicillin/streptomycin (Euroclone) and maintained at 37 °C in 5% CO_2.
The treatment of NIH3T3 in low serum condition was performed by using DMEM supplemented with 2% FBS or 0,25% BSA.
The osteogenic differentiation capacity of MSCs was assessed at passage 3, we platelet MSCs at density of $2x10^4$ in 24-well and for 7 days we used DMEM supplemented with 10% FBS, Dexametasone (10μM) (Sigma-Aldrich) and L-Ascorbic acid (25mM) (Sigma-Aldrich). After a week, we added to media β-Glycerophosphate disodium salt hydrate (5mM) (Sigma-Aldrich).

We treated MSCs for 21 days, then, to detect osteogenic differentiation, Alkaline Phosphatase, Leukocye Kit (Sigma-Aldrich) was used to assess ALP activity, according to manufacturer's instruction, while mineralization was evaluated by staining calcium deposition with Alizarin Red (Sigma-Aldrich).
Human primary monocytes were isolated from healthy-donor bone marrow by centrifugation on Histopaque 1077 (Sigma-Aldrich) and cultured in 96-multiwell plates for 2 weeks to assess osteoclastogenesis. Monocytes were treated with 20 ng/ml macrophage colony stimulation factor (MCSF) (Tebubio) to induce proliferation, and with 20 ng/ml MCSF and 30 ng/ml RANKL (Tebubio) to induce osteoclasts formation. Acid Phosphatase, Leukocyte (TRAP) kit (Sigma-Aldrich) was used to assess TRAP activity, according to manufacturer's instructions.
For pharmacological treatment, Saos-2, HOS and 143B cell lines were treated with 20μM of Y-27632 (Sigma-Aldrich) for 24h.

6.2 EV collection

Osteosarcoma cell lines were platelet at density of $2x10^6$ in T75 flasks. In the conditioned medium experiments, to remove endogenous EVs, FBS added to DMEM medium was ultracentrifuged at 100,000 g by Optima XPN-100 Ultracentrifuge (Beckman Coulter) before use. The media were collected after 24h of conditioning, centrifuged 1,500rpm for 10 min to eliminate cell debris and split in 3 equal amounts to test 3 different isolation protocols: (i) the medium was ultracentrifuged at 100,000*g* for 1h at 4°C to collect EVs on the bottom of tube; (ii) the medium was concentrated by centrifugation for 20 min at 2,000*g* in sterile hydrated 30 kDa MWCO Amicon Ultra Centrifugal filters (Millipore); (iii) the medium was incubated in a ratio of 1:10 with ExoQuick™, according to the manufacturer's instructions.

6.3 Stainings and confocal microscopy analysis

Osteosarcoma cell lines were stained with CFSE (1mM) (Life Technologies) and PKH-26 (Sigma-Aldrich) dyes, according to the manufacturer's instruction.

To visualize actin, cell lines were fixed with 4% paraformaldehyde and incubated with rhodamine-conjugated phalloidin, using Hoechst to stain nuclei.

The confocal microscopy imaging was performed on a Leica TCS-SP8X laser-scanning confocal microscope (Leica Mycrosystem, Mannheim,Germany) equipped with tunable white light laser (WLL) sourse, 405nm diode laser, 3 Internal Spectral Detector Channel (PMT) and 2 Internal Spectral Detector Channels (HyD) GaAsP. Sequential confocal images are acquired using a HCPLAPO 63x oil-immersion objective with a 1024x1024 format, scan speed 400Hz, and z-step size of 0.25 μm. Z-reconstructions are imported into LASX 3D Analysis (Leica Microsystems) software to obtain the three-dimensional surface rendering.

6.4 Flowcytometric analysis

To visualize EVs, we used nanobeads (Spherotech) with known size of 0.5, 0.7 and 1.3 μm to create the gate in which visualize EVs. Moreover, we used 5.000 CountBright™ Absolute Counting Beads (Life Technologies) to evaluate the same volume (5μl) for each samples. EVs, NIH3T3 and osteosarcoma cell lines were analysed with FACSAria II flow cytometer (BD PharMigen) and data were calculated using the FACSDiva software (Tree Star,Inc.).

Primary antibodies: anti human CD63-Alexa Fluor 488, anti human RANK-PE conjugated and anti human RANKL-PE conjugated were purchased by Thermo Fisher Scientific, anti human MCSF-PE conjugated was by R&D SYSTEMS®.

6.5 EV quantities analysis

EXOCET

To quantify isolated EVs, we used EXOCET (SBI,System Biosciences) according to the manufacturer's instructions. This is a quantification assay kit designed as a direct measurement of esterase activity known to be within EVs.

Tunable Resistive Pulse Sensing (TRPS) Technology.

The isolated EVs were resuspended in 150µl of PBS. TRPS analysis were performed by *Izon Science* that provided information about amount of particles/ml for each analysed sample and their size range.

6.6 Western Blotting

NIH3T3 and EV pellet were collected and total protein extraction was performed by homogenizing cells in Ripa lysis buffer (Cell Signalling Technology) containing 1X protease and phosphatase inhibitors cocktail. The homogenates were then centrifuged at 13,000 rpm at +4° for 10 minutes and the resulting supernatant was taken as protein sample. Cell and EV extracts were quantified using the BCA™ Protein Assay (Thermo Scientific). Samples were then diluted in the sample buffer (200 mM Tris-HCl (pH 6.8), 20% β-mercaptoethanol,4% sodium dodecyl sulphate, and bromophenol blue) and resolved in SDS-PAGE, then transferred and immobilized onto nitrocellulose membranes (Amersham). The membranes were blocked using 5% BSA for 30 min and incubated with the appropriate primary and secondary antibodies. Signal intensity was measured with a ChemiDoc Imaging System (BioRad).

Primary antibodies: anti AKT, pAKT, ERK1/2, pERK1/2 were from Cell Signalling Technology; anti GAPDH were supplied by Sigma-Aldrich; anti CD63 were from Thermo Fisher Scientific.

6.7 Apoptosis analysis

Cells were harvested by trypsinization, washed with PBS, then stained with a solution containing 1 mg/ml Propidium Iodide (PI). Apoptosis was analyzed with an APC Annexin V Apoptosis Detection Kit (BD Pharmingen, BD Biosciences) according to the manufacturer's instructions. The fluorescent intensity was measured by BD FACSCanto Flow Cytometer (BD Biosciences). Resulting Annexin distributions were analysed for the proportions of cells defined as Live, Early apoptosis, Late apoptosis and Death.

6.8 Cell cycle analysis

Cell cycle phase distribution was analyzed by flow cytometry using Propidium Iodide (PI) staining. Briefly, NIH3T3 cells were harvested by trypsinization, washed with PBS, then fixed in a solution of a cold 4:1 methanol/acetone solution. Cells were then stained with a solution containing 100μg/ml PI and 0.1 mg/ml RNase A. Stained nuclei were analysed for DNA-PI fluorescence using a Becton Dickinson FACSCanto flow cytometer. Resulting DNA distributions were analysed for the proportions of cells in G0-G1, S and G2-M phases of the cell cycle.

6.9 Wound healing assay

NIH3T3 and human osteoblasts were platelet at density of $3x10^5$/ml in Culture-Inserts (Ibidi), then removed after 24h. Following 5h of EV treatment, cells were fixed with 4% paraformaldehyde, stained with the nuclear dye Hoechst and the wound size was analysed using ImageJ software.

6.10 Soft agar assay

Anchorage-independent growth was determined by soft agar assay. A base layer of complete culture medium in 1% agar was established in 12-well. NIH3T3 cells were plated at $1x10^4$ cells per well in the top layer composed of the same culture medium and 0,7% agar mixture. Growth medium and the treatment with

osteosarcoma-derived-EV was refreshed every 2-3 days. After 30 days, colonies were counted under a light microscope (10X).

6.11 RT–PCR

Total RNA was extracted from cultured cells using the standard Trizol procedure. Each RNA sample was quantified by NanoDrop 2000 (Thermo Scientific). Two µg of RNA were reverse transcribed using the SuperScript™ II Reverse Transcriptase (Invitrogen) to generate cDNA. These were carried out in a final volume of 20 µl containing 100 µM of each primer and *REDTaq®Ready Mix* (Sigma-Aldrich). *Gapdh* was used as housekeeping. PCR-amplified products were analysed on 2% agarose gel containing Gel Red (Biotium), signal intensity was measured with a ChemiDoc Imaging System and densitometry analysis performed by the Quantity One Software (BioRad).

Primer pairs 5'-3':

mouse GAPDH reverse: TGAAGGGGTCGTTGATGGC
mouse GAPDH forward: CCTCGTCCCGTAGACAAAATG
mouse ALP reverse: TGACGTTCCGATCCTGAGTG
mouse ALP forward: TGGTCACAGCAGTTGGTAGC
mouse MMP-9 reverse: GCGGTACAAGTATGCCTCTGC
mouse MMP-9 forward: CAAAGGCAGCGTTAGCCAGA
human GAPDH reverse: GACAAGCTTCCCGTTCTCAG
human GAPDH forward: ACAGTCAGCCGCATCTTCTT
human ALP reverse: CCACCAAATGTGAAGACGTG
human ALP forward: GGACATGCAGTACGAGCTGA
human COLL1A2 reverse: GGCGTGATGGCTTATTTGTT
human COLL1A2 forward: CTGCAAGAACAGCATTGCAT
human RUNX2 reverse: TATGGAGTGCTGCTGGTCTG
human RUNX2 forward: TTACTTACACCCCGCCAGTC
human TNF-α reverse: AGGCCCCAGTTTGAATTCTT
human TNF-α forward: TCCTTCAGACACCCTCAACC
human TGF-β reverse: CCGGTAGTGAACCCGTTGAT
human TGF-β forward: TACCTGAACCCGTGTTGCTC
human IL6 reverse: CAGGGGTGGTTATTGCATCT
human IL6 forward: AAAGAGGCACTGGCAGAAAA

7. References

1. Sommerfeldt DW, Rubin CT. Biology of bone and how it orchestrates the form and function of the skeleton. *Eur. Spine J.* 2001;10 Suppl 2;S86-S95.

2. Miller EJ, Martin GR. The collagen of bone. *Clin. Orthop. Relat Res* 1968;59;195-232.

3. Jiang Y, Jahagirdar BN, Reinhardt RL *et al.* Pluripotency of mesenchymal stem cells derived from adult marrow. *Nature* 2002;418;41-49.

4. Suda T, Takahashi N, Udagawa N, Jimi E, Gillespie MT, Martin TJ. Modulation of osteoclast differentiation and function by the new members of the tumor necrosis factor receptor and ligand families. *Endocr. Rev.* 1999;20;345-357.

5. Parfitt AM. Problems in the application of in vitro systems to the study of human bone remodeling. *Calcif. Tissue Int.* 1995;56 Suppl 1;S5-S7.

6. Shin CS, Lecanda F, Sheikh S, Weitzmann L, Cheng SL, Civitelli R. Relative abundance of different cadherins defines differentiation of mesenchymal precursors into osteogenic, myogenic, or adipogenic pathways. *J. Cell Biochem.* 2000;78;566-577.

7. Teitelbaum SL, Ross FP. Genetic regulation of osteoclast development and function. *Nat. Rev. Genet.* 2003;4;638-649.

8. Teitelbaum SL, Abu-Amer Y, Ross FP. Molecular mechanisms of bone resorption. *J. Cell Biochem.* 1995;59;1-10.

9. Roodman GD. Cell biology of the osteoclast. *Exp. Hematol.* 1999;27;1229-1241.

10. Roodman GD. Mechanisms of bone metastasis. *N. Engl. J. Med.* 2004;350;1655-1664.

11. Troen BR. Molecular mechanisms underlying osteoclast formation and activation. *Exp. Gerontol.* 2003;38;605-614.

12. Delaisse JM, Andersen TL, Engsig MT, Henriksen K, Troen T, Blavier L. Matrix metalloproteinases (MMP) and cathepsin K contribute differently to osteoclastic activities. *Microsc. Res Tech.* 2003;61;504-513.

13. Dempster DW, Hughes-Begos CE, Plavetic-Chee K *et al.* Normal human osteoclasts formed from peripheral blood monocytes express PTH type 1 receptors and are stimulated by PTH in the absence of osteoblasts. *J. Cell Biochem.* 2005;95;139-148.

14. Reddy SV. Regulatory mechanisms operative in osteoclasts. *Crit Rev. Eukaryot. Gene Expr.* 2004;14;255-270.

15. Baron R, Vignery A TVP. The significance of lacunar erosion without osteoclasts: Studies on the reversal phase of the remodeling sequence. *Metab Bone Dis Rel Res* 1980;2S;35-40.

16. Anderson HC. Matrix vesicles and calcification. *Curr. Rheumatol. Rep.* 2003;5;222-226.

17. Frost HM. The skeletal intermediary organization. *Metab Bone Dis. Relat Res.* 1983;4;281-290.

18. Hansen MF, Nellissery MJ, Bhatia P. Common mechanisms of osteosarcoma and Paget's disease. *J. Bone Miner. Res.* 1999;14 Suppl 2;39-44.

19. Hansen MF, Seton M, Merchant A. Osteosarcoma in Paget's disease of bone. *J. Bone Miner. Res.* 2006;21 Suppl 2;58-63.

20. Bacci G, Longhi A, Bertoni F *et al.* Primary high-grade osteosarcoma: comparison between preadolescent and older patients. *J. Pediatr. Hematol. Oncol.* 2005;27;129-134.

21. Bacci G, Balladelli A, Palmerini E *et al.* Neoadjuvant chemotherapy for osteosarcoma of the extremities in preadolescent patients: the Rizzoli Institute experience. *J. Pediatr. Hematol. Oncol.* 2008;30;908-912.

22. Goyal S, Roscoe J, Ryder WD, Gattamaneni HR, Eden TO. Symptom interval in young people with bone cancer. *Eur. J. Cancer* 2004;40;2280-2286.

23. Kansara M, Thomas DM. Molecular pathogenesis of osteosarcoma. *DNA Cell Biol.* 2007;26;1-18.

24. Pakos EE, Nearchou AD, Grimer RJ *et al.* Prognostic factors and outcomes for osteosarcoma: an international collaboration. *Eur. J. Cancer* 2009;45;2367-2375.

25. Williams RF, Fernandez-Pineda I, Gosain A. Pediatric Sarcomas. *Surg. Clin. North Am.* 2016;96;1107-1125.

26. Bielack SS, Kempf-Bielack B, Delling G *et al.* Prognostic factors in high-grade osteosarcoma of the extremities or trunk: an analysis of 1,702 patients treated on neoadjuvant cooperative osteosarcoma study group protocols. *J. Clin. Oncol.* 2002;20;776-790.

27. Andreou D, Bielack SS, Carrle D *et al.* The influence of tumor- and treatment-related factors on the development of local recurrence in osteosarcoma after adequate surgery. An analysis of 1355 patients treated on neoadjuvant Cooperative Osteosarcoma Study Group protocols. *Ann. Oncol.* 2011;22;1228-1235.

28. Goorin AM, Schwartzentruber DJ, Devidas M *et al.* Presurgical chemotherapy compared with immediate surgery and adjuvant chemotherapy for nonmetastatic osteosarcoma: Pediatric Oncology Group Study POG-8651. *J. Clin. Oncol.* 2003;21;1574-1580.

29. Reya T, Morrison SJ, Clarke MF, Weissman IL. Stem cells, cancer, and cancer stem cells. *Nature* 2001;414;105-111.

30. Deng ZL, Sharff KA, Tang N *et al.* Regulation of osteogenic differentiation during skeletal development. *Front Biosci.* 2008;13;2001-2021.

31. Wagner ER, Luther G, Zhu G *et al.* Defective osteogenic differentiation in the development of osteosarcoma. *Sarcoma.* 2011;2011;325238.

32. Cheng H, Jiang W, Phillips FM *et al.* Osteogenic activity of the fourteen types of human bone morphogenetic proteins (BMPs). *J. Bone Joint Surg. Am.* 2003;85-A;1544-1552.

33. Luo X, Chen J, Song WX *et al.* Osteogenic BMPs promote tumor growth of human osteosarcomas that harbor differentiation defects. *Lab Invest* 2008;88;1264-1277.

34. Wagner ER, Luther G, Zhu G *et al.* Defective osteogenic differentiation in the development of osteosarcoma. *Sarcoma.* 2011;2011;325238.

35. Thomas DM, Johnson SA, Sims NA *et al.* Terminal osteoblast differentiation, mediated by runx2 and p27KIP1, is disrupted in osteosarcoma. *J. Cell Biol.* 2004;167;925-934.

36. Lonardo F, Ueda T, Huvos AG, Healey J, Ladanyi M. p53 and MDM2 alterations in osteosarcomas: correlation with clinicopathologic features and proliferative rate. *Cancer* 1997;79;1541-1547.

37. Miller CW, Aslo A, Won A, Tan M, Lampkin B, Koeffler HP. Alterations of the p53, Rb and MDM2 genes in osteosarcoma. *J. Cancer Res. Clin. Oncol.* 1996;122;559-565.

38. Yoshida A, Ushiku T, Motoi T *et al.* Immunohistochemical analysis of MDM2 and CDK4 distinguishes low-grade osteosarcoma from benign mimics. *Mod. Pathol.* 2010;23;1279-1288.

39. Yoshida A, Ushiku T, Motoi T *et al.* MDM2 and CDK4 immunohistochemical coexpression in high-grade osteosarcoma: correlation with a dedifferentiated subtype. *Am. J. Surg. Pathol.* 2012;36;423-431.

40. Jeon DG, Koh JS, Cho WH *et al.* Clinical outcome of low-grade central osteosarcoma and role of CDK4 and MDM2 immunohistochemistry as a diagnostic adjunct. *J. Orthop. Sci.* 2015;20;529-537.

41. Berman SD, Calo E, Landman AS *et al.* Metastatic osteosarcoma induced by inactivation of Rb and p53 in the osteoblast lineage. *Proc. Natl. Acad. Sci. U. S. A* 2008;105;11851-11856.

42. Feugeas O, Guriec N, Babin-Boilletot A *et al.* Loss of heterozygosity of the RB gene is a poor prognostic factor in patients with osteosarcoma. *J. Clin. Oncol.* 1996;14;467-472.

43. Bianchi E, Artico M, Di Cristofano C *et al.* Growth factors, their receptor expression and markers for proliferation of endothelial and neoplastic cells in human osteosarcoma. *Int. J. Immunopathol. Pharmacol.* 2013;26;621-632.

44. Zhang H, Wu H, Zheng J *et al.* Transforming growth factor beta1 signal is crucial for dedifferentiation of cancer cells to cancer stem cells in osteosarcoma. *Stem Cells* 2013;31;433-446.

45. Chen J, Song Y, Yang J *et al.* The up-regulation of cysteine-rich protein 61 induced by transforming growth factor beta enhances osteosarcoma cell migration. *Mol. Cell Biochem.* 2013;384;269-277.

46. Denduluri SK, Wang Z, Yan Z *et al.* Molecular pathogenesis and therapeutic strategies of human osteosarcoma. *J. Biomed. Res.* 2015;30.

47. Salvatore V, Focaroli S, Teti G, Mazzotti A, Falconi M. Changes in the gene expression of co-cultured human fibroblast cells and osteosarcoma cells: the role of microenvironment. *Oncotarget.* 2015;6;28988-28998.

48. Hess C, Sadallah S, Hefti A, Landmann R, Schifferli JA. Ectosomes released by human neutrophils are specialized functional units. *J. Immunol.* 1999;163;4564-4573.

49. Cocucci E, Racchetti G, Meldolesi J. Shedding microvesicles: artefacts no more. *Trends Cell Biol.* 2009;19;43-51.

50. Gyorgy B, Szabo TG, Pasztoi M *et al.* Membrane vesicles, current state-of-the-art: emerging role of extracellular vesicles. *Cell Mol. Life Sci.* 2011;68;2667-2688.

51. Trams EG, Lauter CJ, Salem N, Jr., Heine U. Exfoliation of membrane ecto-enzymes in the form of micro-vesicles. *Biochim. Biophys. Acta* 1981;645;63-70.

52. Harding C, Heuser J, Stahl P. Endocytosis and intracellular processing of transferrin and colloidal gold-transferrin in rat reticulocytes: demonstration of a pathway for receptor shedding. *Eur. J. Cell Biol.* 1984;35;256-263.

53. Raposo G, Stoorvogel W. Extracellular vesicles: exosomes, microvesicles, and friends. *J. Cell Biol.* 2013;200;373-383.

54. Simons M, Raposo G. Exosomes--vesicular carriers for intercellular communication. *Curr. Opin. Cell Biol.* 2009;21;575-581.

55. Thery C, Ostrowski M, Segura E. Membrane vesicles as conveyors of immune responses. *Nat. Rev. Immunol.* 2009;9;581-593.

56. Ronquist G, Brody I. The prostasome: its secretion and function in man. *Biochim. Biophys. Acta* 1985;822;203-218.

57. Park KH, Kim BJ, Kang J *et al.* Ca2+ signaling tools acquired from prostasomes are required for progesterone-induced sperm motility. *Sci. Signal.* 2011;4;ra31.

58. Aalberts M, Dissel-Emiliani FM, van Adrichem NP *et al.* Identification of distinct populations of prostasomes that differentially express prostate stem cell antigen, annexin A1, and GLIPR2 in humans. *Biol. Reprod.* 2012;86;82.

59. Caby MP, Lankar D, Vincendeau-Scherrer C, Raposo G, Bonnerot C. Exosomal-like vesicles are present in human blood plasma. *Int. Immunol.* 2005;17;879-887.

60. Pisitkun T, Shen RF, Knepper MA. Identification and proteomic profiling of exosomes in human urine. *Proc. Natl. Acad. Sci. U. S. A* 2004;101;13368-13373.

61. Ogawa Y, Miura Y, Harazono A *et al.* Proteomic analysis of two types of exosomes in human whole saliva. *Biol. Pharm. Bull.* 2011;34;13-23.

62. Admyre C, Johansson SM, Qazi KR *et al.* Exosomes with immune modulatory features are present in human breast milk. *J. Immunol.* 2007;179;1969-1978.

63. Asea A, Jean-Pierre C, Kaur P *et al.* Heat shock protein-containing exosomes in mid-trimester amniotic fluids. *J. Reprod. Immunol.* 2008;79;12-17.

64. Andre F, Schartz NE, Movassagh M *et al.* Malignant effusions and immunogenic tumour-derived exosomes. *Lancet* 2002;360;295-305.

65. Vella LJ, Sharples RA, Lawson VA, Masters CL, Cappai R, Hill AF. Packaging of prions into exosomes is associated with a novel pathway of PrP processing. *J. Pathol.* 2007;211;582-590.

66. Masyuk AI, Huang BQ, Ward CJ *et al.* Biliary exosomes influence cholangiocyte regulatory mechanisms and proliferation through interaction with primary cilia. *Am. J. Physiol Gastrointest. Liver Physiol* 2010;299;G990-G999.

67. Heijnen HF, Schiel AE, Fijnheer R, Geuze HJ, Sixma JJ. Activated platelets release two types of membrane vesicles: microvesicles by surface shedding and exosomes derived from exocytosis of multivesicular bodies and alpha-granules. *Blood* 1999;94;3791-3799.

68. Deregibus MC, Cantaluppi V, Calogero R *et al.* Endothelial progenitor cell derived microvesicles activate an angiogenic program in endothelial cells by a horizontal transfer of mRNA. *Blood* 2007;110;2440-2448.

69. Muralidharan-Chari V, Clancy J, Plou C *et al.* ARF6-regulated shedding of tumor cell-derived plasma membrane microvesicles. *Curr. Biol.* 2009;19;1875-1885.

70. Booth AM, Fang Y, Fallon JK, Yang JM, Hildreth JE, Gould SJ. Exosomes and HIV Gag bud from endosome-like domains of the T cell plasma membrane. *J. Cell Biol.* 2006;172;923-935.

71. Bobrie A, Colombo M, Raposo G, Thery C. Exosome secretion: molecular mechanisms and roles in immune responses. *Traffic.* 2011;12;1659-1668.

72. Thery C, Amigorena S, Raposo G, Clayton A. Isolation and characterization of exosomes from cell culture supernatants and biological fluids. *Curr. Protoc. Cell Biol.* 2006;Chapter 3;Unit.

73. Raposo G, Nijman HW, Stoorvogel W *et al.* B lymphocytes secrete antigen-presenting vesicles. *J. Exp. Med.* 1996;183;1161-1172.

74. Escola JM, Kleijmeer MJ, Stoorvogel W, Griffith JM, Yoshie O, Geuze HJ. Selective enrichment of tetraspan proteins on the internal vesicles of multivesicular endosomes and on exosomes secreted by human B-lymphocytes. *J. Biol. Chem.* 1998;273;20121-20127.

75. Van Niel G, Mallegol J, Bevilacqua C *et al.* Intestinal epithelial exosomes carry MHC class II/peptides able to inform the immune system in mice. *Gut* 2003;52;1690-1697.

76. Wubbolts R, Leckie RS, Veenhuizen PT *et al.* Proteomic and biochemical analyses of human B cell-derived exosomes. Potential implications for their function and multivesicular body formation. *J. Biol. Chem.* 2003;278;10963-10972.

77. Soo CY, Song Y, Zheng Y *et al.* Nanoparticle tracking analysis monitors microvesicle and exosome secretion from immune cells. *Immunology* 2012;136;192-197.

78. Hemler ME. Tetraspanin proteins mediate cellular penetration, invasion, and fusion events and define a novel type of membrane microdomain. *Annu. Rev. Cell Dev. Biol.* 2003;19;397-422.

79. Ratajczak J, Wysoczynski M, Hayek F, Janowska-Wieczorek A, Ratajczak MZ. Membrane-derived microvesicles: important and underappreciated mediators of cell-to-cell communication. *Leukemia* 2006;20;1487-1495.

80. Valadi H, Ekstrom K, Bossios A, Sjostrand M, Lee JJ, Lotvall JO. Exosome-mediated transfer of mRNAs and microRNAs is a novel mechanism of genetic exchange between cells. *Nat. Cell Biol.* 2007;9;654-659.

81. Skog J, Wurdinger T, van Rijn S *et al.* Glioblastoma microvesicles transport RNA and proteins that promote tumour growth and provide diagnostic biomarkers. *Nat. Cell Biol.* 2008;10;1470-1476.

82. Hunter MP, Ismail N, Zhang X *et al.* Detection of microRNA expression in human peripheral blood microvesicles. *PLoS. One.* 2008;3;e3694.

83. Rabinowits G, Gercel-Taylor C, Day JM, Taylor DD, Kloecker GH. Exosomal microRNA: a diagnostic marker for lung cancer. *Clin. Lung Cancer* 2009;10;42-46.

84. Michael A, Bajracharya SD, Yuen PS *et al.* Exosomes from human saliva as a source of microRNA biomarkers. *Oral Dis.* 2010;16;34-38.

85. Mittelbrunn M, Gutierrez-Vazquez C, Villarroya-Beltri C *et al.* Unidirectional transfer of microRNA-loaded exosomes from T cells to antigen-presenting cells. *Nat. Commun.* 2011;2;282.7

86. Montecalvo A, Larregina AT, Shufesky WJ *et al.* Mechanism of transfer of functional microRNAs between mouse dendritic cells via exosomes. *Blood* 2012;119;756-766.

87. Bellingham SA, Coleman BM, Hill AF. Small RNA deep sequencing reveals a distinct miRNA signature released in exosomes from prion-infected neuronal cells. *Nucleic Acids Res.* 2012;40;10937-10949.

88. Nolte-'t Hoen EN, Buermans HP, Waasdorp M, Stoorvogel W, Wauben MH, 't Hoen PA. Deep sequencing of RNA from immune cell-derived vesicles uncovers the selective incorporation of small non-coding RNA biotypes with potential regulatory functions. *Nucleic Acids Res.* 2012;40;9272-9285.

89. Eldh M, Lotvall J, Malmhall C, Ekstrom K. Importance of RNA isolation methods for analysis of exosomal RNA: evaluation of different methods. *Mol. Immunol.* 2012;50;278-286.

90. Witwer KW, Buzas EI, Bemis LT *et al.* Standardization of sample collection, isolation and analysis methods in extracellular vesicle research. *J. Extracell. Vesicles.* 2013;2.

91. Antonyak MA, Li B, Boroughs LK *et al.* Cancer cell-derived microvesicles induce transformation by transferring tissue transglutaminase and fibronectin to recipient cells. *Proc. Natl. Acad. Sci. U. S. A* 2011;108;4852-4857.

92. Colombo M, Raposo G, Thery C. Biogenesis, secretion, and intercellular interactions of exosomes and other extracellular vesicles. *Annu. Rev. Cell Dev. Biol.* 2014;30;255-289.

93. Zhang HG, Grizzle WE. Exosomes: a novel pathway of local and distant intercellular communication that facilitates the growth and metastasis of neoplastic lesions. *Am. J. Pathol.* 2014;184;28-41.

94. Rosner H. Significance of gangliosides in neuronal differentiation of neuroblastoma cells and neurite growth in tissue culture. *Ann. N. Y. Acad. Sci.* 1998;845;200-214.

95. Hoon DS, Kuo CT, Wen S *et al.* Ganglioside GM2/GD2 synthetase mRNA is a marker for detection of infrequent neuroblastoma cells in bone marrow. *Am. J. Pathol.* 2001;159;493-500.

96. Marimpietri D, Petretto A, Raffaghello L *et al.* Proteome profiling of neuroblastoma-derived exosomes reveal the expression of proteins potentially involved in tumor progression. *PLoS. One.* 2013;8;e75054.

97. Roth M, Linkowski M, Tarim J *et al.* Ganglioside GD2 as a therapeutic target for antibody-mediated therapy in patients with osteosarcoma. *Cancer* 2014;120;548-554.

98. Antonyak MA, Cerione RA. Microvesicles as mediators of intercellular communication in cancer. *Methods Mol. Biol.* 2014;1165;147-173.

99. D'Asti E, Chennakrishnaiah S, Lee TH, Rak J. Extracellular Vesicles in Brain Tumor Progression. *Cell Mol. Neurobiol.* 2016;36;383-407.

100. Martin JW, Zielenska M, Stein GS, van Wijnen AJ, Squire JA. The Role of RUNX2 in Osteosarcoma Oncogenesis. *Sarcoma.* 2011;2011;282745.

101. Poon VI, Roth M, Piperdi S *et al.* Ganglioside GD2 expression is maintained upon recurrence in patients with osteosarcoma. *Clin. Sarcoma. Res.* 2015;5;4.

102. Lo Piccolo MS, Cheung NK, Cheung IY. GD2 synthase: a new molecular marker for detecting neuroblastoma. *Cancer* 2001;92;924-931.

103. Zucchini C, Manara MC, Pinca RS *et al.* CD99 suppresses osteosarcoma cell migration through inhibition of ROCK2 activity. *Oncogene* 2014;33;1912-1921.

104. Li B, Antonyak MA, Zhang J, Cerione RA. RhoA triggers a specific signaling pathway that generates transforming microvesicles in cancer cells. *Oncogene* 2012;31;4740-4749.

105. Bernardo ME, Zaffaroni N, Novara F *et al.* Human bone marrow derived mesenchymal stem cells do not undergo transformation after long-term in vitro culture and do not exhibit telomere maintenance mechanisms. *Cancer Res.* 2007;67;9142-9149.